SUPPORTING INFORMATION

Dextran-Functionalized Semiconductor Quantum Dot Bioconjugates for Bioanalysis and Imaging

Kelly Rees,[#] Michael V. Tran,[#] Melissa Massey, Hyungki Kim, Katherine D. Krause, W. Russ Algar**

Department of Chemistry, 2036 Main Mall, Vancouver, British Columbia, V6T 1Z1, Canada.

[#] KR and MVT contributed equally.

* Corresponding authors: mmassey@chem.ubc.ca (MM), algar@chem.ubc.ca (WRA)

Table of Contents

List of Schemes

List of Figures

List of Tables

Supplementary Experimental Methods

Additional Materials. *N*, *N*′-diisopropylcarbodiimide (DIC; 99%), 2-propanol (≥99.5%), dimethyl sulfoxide (DMSO; ≥99.9%), ethylenediamine (≥99%), dichloromethane (DCM; ≥99.5%), sodium hydroxide (≥97%), hexamethylenediamine (HMDA; 98%), sodium cyanoborohydride (95%), sodium (meta)periodate (≥99%), hydrochloric acid (ACS reagent, 37%), L-glutathione reduced (≥98.8%), L-histidine (≥99%), methanol (≥99.8%), chloroform (≥99.8%), tetramethylammonium hydroxide solution (TMAH; 25 wt% in methanol), tris(2-carboxyethyl) phosphine hydrochloride (TCEP, ≥98%), agarose, fluorescein isothiocyanate isomer I (FITC; ≥90%), fluorescein, rhodamine B, 1-(3-aminopropyl)imidazole (API), ethanolamine (ACS reagent, >99%), 5,5'-dithiobis(2-nitrobenzoic acid) (DTNB), anthrone (ACS reagent, 97%), sulfuric acid (95–98%), and Concanavalin A (ConA) were from Sigma-Aldrich (Oakville, ON, Canada). Glucose was from BDH Chemicals (Toronto, ON, Canada). Potassium permanganate was from Anachemia Science (Richmond, BC, Canada). Ninhydrin monohydrate was from Amresco (Dallas, TX). 5-(1,2-dithiolan-3-yl)pentanoic acid (lipoic acid, LA) was from Oakwood Chemical (Estill, SC). *N*-hydroxysuccinimide (NHS), anhydrous sodium sulfate, and tetrahydrofuran (THF) were from EMD Millipore (Burlington, MA). 2,4,6-trinitrobenzene sulfonic acid (TNBS; 1% in MeOH) was from G-Biosciences (St. Louis, MO). ConA-sepharose 4B was from GE Healthcare Life Sciences (Chicago, IL).

Water (sterile, nuclease free; defined as ultrapure H_2O or UPH_2O) and glycerol (sterile) were from VWR International (Mississauga, ON, Canada). Water was from a Milli-Q system (Millipore Sigma, Burlington, MA) and had a specific resistance ≥18 MΩ cm. Unless otherwise specified, *water* refers to that from the Milli-Q system. HEPES was from Sigma-Aldrich (Oakville, ON, Canada). Potassium carbonate anhydrous (ACS grade), sodium bicarbonate (ACS grade), sodium tetraborate decahydrate (ACS grade), and citric acid (ACS grade) were from Amresco (Dallas, TX). Sodium chloride (ACS grade), ethylenediamine tetraacetic acid disodium salt dehydrate (EDTA), magnesium chloride hexahydrate, potassium chloride, tris-borate-EDTA 10× solution, and sodium phosphate dibasic heptahydrate were from Fisher Scientific (Ottawa, ON, Canada). Potassium phosphate monobasic was from EMD Millipore (Burlington, MA).

Calcium chloride dehydrate was from Anachemia Science (Richmond, BC, Canada). Buffers were filtered through a 0.22 μm-porous membrane filter prior to use.

Dextran from *Leuconostoc mesenteroides* (~6000 MW, lot number D-4967A) was from Dextran Products Limited (Scarborough, ON, Canada). Dextran from *Leuconostoc* spp. (M_r ~6000, 4500–7500 Da, product number 31388) and dextran from *Leuconostoc mesenteroides* (average mol wt. 9000–11000 Da, product number D9260) were from Sigma-Aldrich. Monoamine dextran (3.5, 6, and 10 kDa) were from Fina Biosolutions (Rockville, MD) and were used as a starting material in some cases. No differences in the resulting ligands were observed, and so the ligands are differentiated only by the dextran molecular weight and source bacterial strain. The (*L*) and (*M*) notations are used for *Leuconostoc* spp. and *Leuconostoc mesenteroides*, respectively. The purity of the commercial dextran was estimated by ^{1}H NMR to be >99% carbohydrate. The < 1% of small-molecule impurity was removed during ethanol precipitation steps.

Bovine serum albumin (BSA) was from Amresco (Dallas, TX, USA). Lysozyme from chicken egg white and bovine plasma were from Sigma-Aldrich (Oakville, ON, Canada). Skim milk powder was from the local grocer.

Peptides were from Bio-Synthesis Inc. (Lewisville, TX) and labeled with Alexa Fluor dyes (Thermo Fisher Scientific, Carlsbad, CA) as described elsewhere.[1] TPCK-treated trypsin from bovine pancreas was obtained as a lyophilized powder from Sigma Life Sciences (St. Louis, MO). Human plasmin was from Haematologic Technologies, Inc. (Essex Junction, VT).

TAC Anti-EPO and TAC Anti-HER2 complexes were prepared using the EasySep™ Do-It-Yourself Selection Kit (STEMCELL Technologies, Vancouver, BC, Canada). Anti-HER2 antibody (NBP2-32863) was from Novus Biologicals (Burlington, ON, Canada). Anti-EPO antibody (EPO-16, clone 16F1H11, mouse monoclonal antibody to human erythropoietin) was from STEMCELL Technologies. The erythropoietin (EPO) ELISA Kit and lyophilized human recombinant EPO (rhEPO) were from STEMCELL Technologies. rhEPO was reconstituted in sterile water (5 μg/25 μL) and diluted to 1.0 mL with *Buffer B* from the ELISA kit (PBS buffer with additives).

Chloroform-D (D 99.8%) was from Cambridge Isotope Laboratories (Tewksbury, MA). Deuterium oxide (99.9 atom% D) was from Sigma-Aldrich.

Citrate-coated gold nanoparticles (AuNPs, 50 nm) were from Cytodiagnostics (Burlington, ON, Canada).

Instrumentation. UV-visible absorption and photoluminescence (PL) spectra were acquired using an Infinite M1000 Pro plate reader (Tecan Ltd., Morrisville, NC). Brightfield and fluorescence imaging were done with an IX83 inverted epifluorescence microscope (Olympus, Richmond Hill, ON, Canada) equipped with an X-Cite 120XL metal-halide light source (Excelitas Technologies, Mississauga, ON, Canada), an Orca-Flash 4.0 V2 sCMOS camera (C11440; Hamamatsu Photonics, Hamamatsu, SZK, Japan), motorized filter wheels (Sutter Instruments, Novato, CA), and MetaMorph/MetaFluor software (Molecular Devices, Sunnyvale, CA). For cell immunolabeling, the filter set was 405/20 (center line/bandwidth in nm) for the excitation filter, a 590 nm cut-off dichroic mirror, and a 600 nm longpass emission filter. For cellular microinjection, the filter set was 405/20 (center line/bandwidth in nm) for the excitation filter, a 565 nm cut-off dichroic mirror, and a 570 nm longpass emission filter. Filters and dichroic mirrors were from Chroma Technology Corp (Bellow Falls, VT, USA). ImageJ software (NIH, Bethesda, MD) was used for processing images.

NMR spectra were collected with a Bruker AV III HD 400 MHz spectrometer (Bruker, Billerica, MA). IR spectra were acquired using a Frontier FT-IR spectrometer with attenuated total reflectance (ATR) sampling and a ZnSe ATR crystal, with data collected over the wavenumber range of 4000 to 650 cm^{-1} (PerkinElmer, Waltham, MA, USA). Electrospray ionization (ESI) mass spectra were obtained using a Waters ZQ mass spectrometer (Milford, MA). Unless otherwise noted, agarose gels were imaged using a Gel Doc XR+ System (Bio-Rad Laboratories Inc., Hercules, CA).

Dynamic light scattering (DLS) measurements were made on a Nanobrook Omni instrument (Brookhaven Instruments Inc., Long Island, NY). Nanoparticle tracking analysis (NTA) was done using a NanoSight NS300 (Malvern Panalytical Ltd., Malvern, Worcestershire, UK). The

source laser was 488 nm and a 500 nm long-pass filter was used to block scattered laser light for fluorescence mode NTA measurements.

Capillary electrophoresis (CE) was performed using an Agilent 7100 CE system (Agilent Technologies, Saint Laurent, QC, Canada) equipped with hydrodynamic injection, a fused silica capillary with an inner diameter of 50 μm, and a diode array detector for UV-visible absorption. The effective length of the capillary was 52 cm. The applied potential was 25 kV with a current of 60 μA.

An InjectMan 4 micromanipulator, FemtoJet 4i microinjector, and Femtotip II needles (Eppendorf, Mississauga, Ontario, Canada) were used for microinjection.

Ligand Synthesis. The following procedures were used to synthesize the ligands depicted in Figure 1 (main text).

2,5-dioxopyrrolidin-1-yl 5-(1,2-dithiolan-3-yl)pentanoate (LA-NHS)

LA-NHS was synthesized (Scheme S1) using a slightly modified literature procedure.[2] LA (2.1 g, 10 mmol) and NHS (1.3 g, 11 mmol) were dissolved in THF (50 mL). DIC (1.7 mL, 12 mmol) was diluted with THF (12 mL) and added in small portions to the reaction mixture. The flask was placed under nitrogen and left to stir for 4 h during which time diisopropylurea precipitated out of solution. Ice-cold isopropanol (100 mL) was added and the precipitate dissolved. The solvent volume was reduced using rotary evaporation and the remaining reaction mixture was cooled at –20 °C overnight, during which time yellow crystals formed. These crystals were collected using vacuum filtration and washed with ice-cold isopropanol before being dried under vacuum. The yellow powder was stored at –20 °C. Crude yield: 2.28 g. ^{1}H NMR ($CDCl_3$, 400 MHz): 3.52–3.64 (m, 1H), 3.06–3.24 (m, 2H), 2.80–2.90 (m, 4H), 2.59–2.67 (m, 2H), 2.43–2.53 (m, 1H), 1.88–1.99 (m, 1H), 1.66–1.85 (m, 4H), 1.49–1.63 (m, 4H)*. The * indicates the presence of an unknown overlapping peak (not from LA-NHS) with an integral of 2H. ESI$^+$ MS (MeOH): m/z 326.1 $[M + Na]^+$ (calculated for $C_{12}H_{17}NO_4S_2Na$ = 326.05).

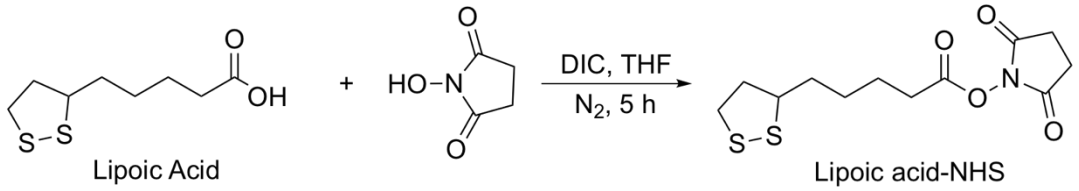

Scheme S1.

N-(2-aminoethyl)-5-(1,2-dithiolan-3-yl)pentanamide (LA-amine)

LA-amine was synthesized (Scheme S2) following a previously published method.[3] Ethylenediamine (10 mL, 0.15 mol) was diluted with DCM (10 mL) and cooled on ice. LA-NHS (0.62 g, 2.0 mmol) was dissolved in DCM (50 mL) and this solution was added dropwise to the cooled and stirred ethylenediamine/DCM mixture over ~2 h. The reaction was then stirred for 3 h at room temperature during which time a precipitate formed. The mixture was washed once with water (75 mL) and three times with a 1 M NaOH/brine mixture (3:2 v/v, 50 mL). The now optically clear and yellow organic phase was dried over sodium sulfate and the solvent volume was reduced under a flow of nitrogen. The product was intentionally not fully dried (it is very susceptible to polymerization) and was instead stored in DCM (*ca.* 10 mg/mL) at 4 °C. Thin-layer chromatography (TLC): DCM/MeOH (9:1 v/v), R_f (LA-amine) = 0.04. TLC plates were visualized under UV light and stained with both $KMnO_4$ and ninhydrin stains. ^{1}H NMR ($CDCl_3$, 400 MHz): 5.90 (br, s, 1H), 3.52–3.63 (m, 1H), 3.30 (q, J = 5.8 Hz, 2H), 3.08–3.23 (m, 2H), 2.87–2.80 (m, 2H), 2.42–2.52 (m, 1H), 2.14–2.24 (m, 2H), 1.84–1.97 (m, 1H), 1.33–1.77 (m, 10H)*. The * indicates the presence of an overlapping peak (not from LA-amine) with an integral of 2H. ESI$^+$ MS (MeOH): m/z 249.3 $[M + H]^+$ (calculated for $C_{10}H_{21}N_2OS_2$ = 249.10).

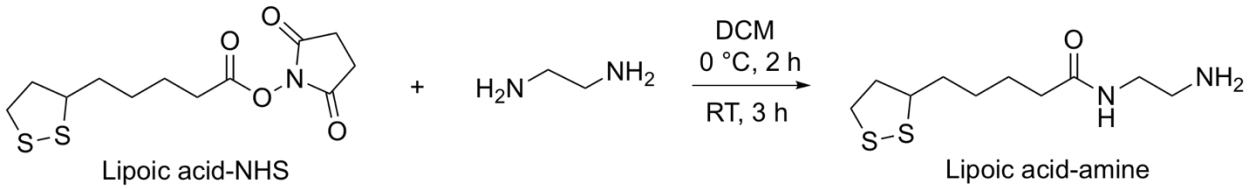

Scheme S2.

Terminal Amine-modified Dextran (D6-t-NH_2)

D6-t-NH_2 was synthesized (Scheme S3) using a procedure modified from previously published methods.[4,5] Dextran from *Leuconostoc* spp. (D6; ~6 kDa MW, 2.0 g, 0.33 mmol) was dissolved

in water (10 mL). HMDA (2.0 mL, 14 mmol) was added and the solution was placed under nitrogen and stirred for 2 h at room temperature. Sodium cyanoborohydride (0.42 g, 6.6 mmol) was added and the solution was stirred overnight under nitrogen. The reaction mixture was split into two centrifuge tubes and the functionalized dextran product was collected via precipitation with EtOH (~35 mL) and centrifugation. The resulting pellets were redissolved in water (~5 mL) and precipitated two further times with EtOH (~35 mL). The pellets were dried under vacuum overnight. The pellets were ground to a fine powder and dried further under vacuum before being stored at room temperature. Crude yield: 1.82 g.

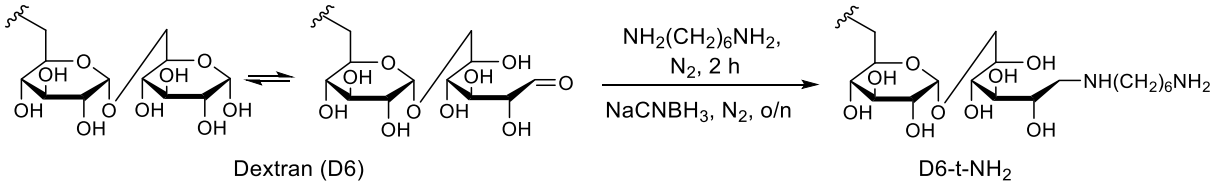

Scheme S3.

This procedure was repeated using dextran from *Leuconostoc mesenteroides* (6 kDa and 9–11 kDa MW). For the larger MW dextran, the quantities were adjusted so that the molar equivalents of reagents was the same as above. The product for the larger MW dextran was also lyophilized rather than dried under vacuum.

Terminal Lipoic Acid-modified Dextran (D6-t-LA)

Terminal lipoic acid-modified dextran was synthesized as shown in Scheme S4. D6-t-NH_2 (1.6 g, 0.26 mmol) and LA-NHS (0.65 g, 2.1 mmol) were dissolved in a mixture of DMSO (16 mL) and UPH_2O (4 mL) forming a pale-yellow solution. The reaction was stirred overnight at room temperature. Bicarbonate buffer (20 mL, 100 mM, pH 9.33) was added and the solution became cloudy. The solution was transferred to a separating funnel and washed three times with DCM (~80 mL). The aqueous phase was collected and DMSO was added until the solution became optically clear. The reaction mixture was split into small portions (~10 mL) and precipitated with EtOH (~35 mL). The functionalized dextran was then collected via centrifugation. The resulting pellets were redissolved in water (~5 mL) and precipitated two further times with EtOH (~35

mL). The pellets were dried under vacuum overnight. The pellets were ground to a fine powder and dried further under vacuum before being stored at –20 °C. Crude yield: 1.42 g.

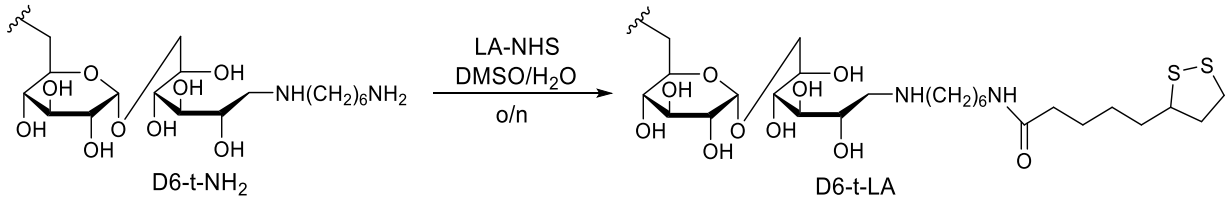

Scheme S4.

This procedure was repeated with different batches of D-t-NH_2, including those prepared with 9–11 kDa MW dextran (D10-t-NH_2), which, as above, was lyophilized rather than dried under vacuum.

Oxidized Dextran (D6-p-CHO)

Dextran was partially oxidized using an adapted method from the literature (Scheme S5).[6] Dextran from *Leuconostoc* spp. (D6; ~6 kDa MW, 4.0 g, 0.67 mmol of polymer chains or ~25 mmol anhydroglucose, AHG) was dissolved in water (20 mL). Sodium (meta)periodate (0.80 g, 3.8 mmol, 15 mol % AHG) was dissolved in water (5 mL) and added to the dextran solution. The mixture was stirred overnight at 4 °C, protected from light. The mixture (~25 mL) was dialyzed (3.5 kDa MWCO membrane, Spectrum Laboratories Inc., Rancho Dominguez, CA) against water (1 L) for 3 days with two water changes. The product was lyophilized to give a fluffy, white compound that was stored at –20 °C. Crude yield: 1.53 g. This product was used to prepare D6-p-NH_2 and D6-p-DHLAm.

A similar procedure was performed to prepare oxidized dextran as a precursor to D6-p-API. Dextran from *Leuconostoc* spp. (D6; ~6 kDa MW, 2.0 g, 0.33 mmol of polymer chains or ~12 mmol AHG) was dissolved in water (50 mL). Sodium (meta)periodate (355 mg, 1.66 mmol, 13.5 mol % AHG) was added and the mixture was stirred overnight at 4 °C. The samples were then dialyzed (3.5 kDa MWCO membrane) against water (1 L) for 24 h with two water changes. The purified samples were lyophilized to yield a fluffy, white solid that was stored at –20 °C.

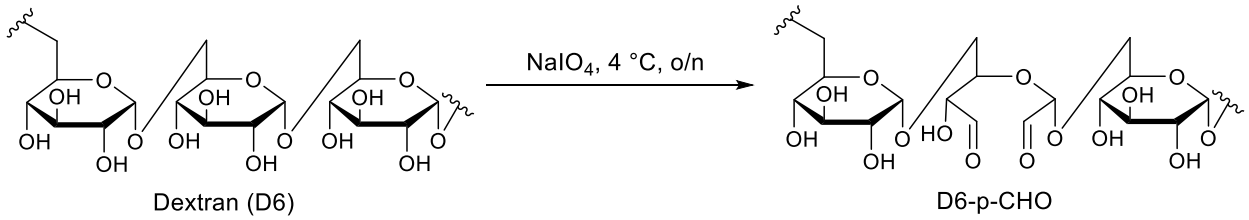

Scheme S5.

Pendant Amine-modified Dextran (D6-p-NH_2)

Pendant amine-modified dextran was synthesized as shown in Scheme S6. D6-p-CHO (0.41g, 68 µmol dextran, maximum 0.68 mmol aldehyde) was dissolved in water (5 mL). HMDA (2.0 mL, 14 mmol) was added to the dextran solution and the mixture was stirred at room temperature for 1.75 h. Sodium cyanoborohydride (0.23 g, 3.7 mmol) was added and the reaction mixture was stirred overnight at room temperature. The reaction mixture was split into two centrifuge tubes and the functionalized-dextran product was collected via precipitation with EtOH (~12 mL) and centrifugation. The resulting pellets were redissolved in water (~2 mL) and precipitated two further times with EtOH (~8 mL). The pellets were dried under vacuum for 2 h. The dried product was stored at room temperature. Crude yield: 0.36 g.

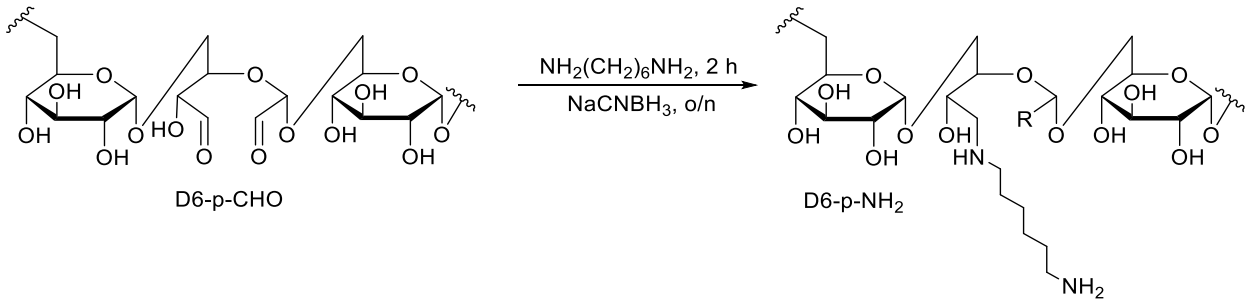

Scheme S6.

Pendant Lipoic Acid-modified Dextran (D6-p-LA)

Pendant LA-modified dextran was synthesized as shown in Scheme S7. D6-p-NH_2 (0.30 g, estimated 46 µmol dextran) and LA-NHS (0.56 g, 1.8 mmol) were dissolved in a mixture of DMSO (8 mL) and water (2 mL) and stirred overnight at room temperature. The reaction mixture was transferred to a separating funnel and bicarbonate buffer (10 mL, 100 mM, pH 9.28) was added, forming a cloudy solution. This solution was washed three times with DCM (40 mL). The organic phase was washed with water (10 mL) and then DMSO was added to the combined

aqueous phases until the solution became optically clear. The reaction mixture was split into small portions (~10 mL) and precipitated with EtOH (~30 mL). The functionalized dextran was then collected via centrifugation. The resulting pellets were redissolved in water (~2 mL) and precipitated two further times with EtOH (~30 mL). The pellets were dried under vacuum for 90 min. The dried product was stored at –20 °C. Crude yield: 0.26 g.

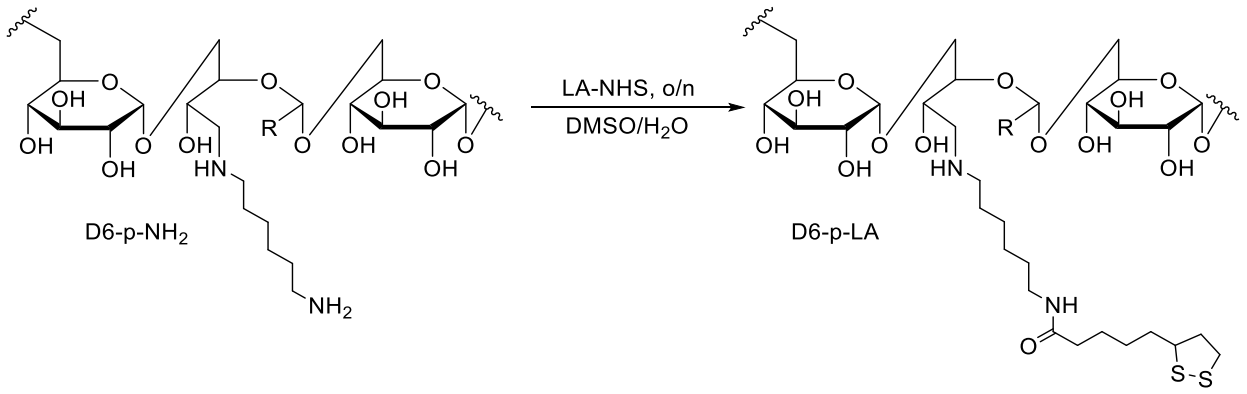

Scheme S7.

Pendant Lipoic Acid-Amine-modified Dextran (D6-p-LAm)

Pendant LA-amine-modified dextran was synthesized as shown in Scheme S8. LA-amine in DCM (18.5 mL, estimated 185 mg, 0.75 mmol) was placed under a flow of nitrogen to reduce the solvent volume to less than 5 mL. DMSO (5 mL) was then added. The remaining DCM was removed under nitrogen. This solution was added to D6-p-CHO (0.41 g, 0.67 μmol dextran) along with additional DMSO (5 mL) and water (2 mL) in order to completely dissolve the dextran. The reaction was stirred at room temperature for 1.25 h before sodium cyanoborohydride (0.24 g, 3.8 mmol) was added. The reaction mixture was stirred overnight at room temperature, then transferred to a separating funnel. Bicarbonate buffer (12 mL, 100 mM, pH 9.28) was added and turned the solution cloudy. The mixture was washed three times with DCM (50 mL). The aqueous phase was diluted with DMSO (50 mL) and 1 M HCl (*aq*) was added dropwise until the solution became clear. The reaction mixture was split into small portions (~15 mL) and precipitated with EtOH (~30 mL). The modified dextran was then collected via centrifugation. The resulting pellets were redissolved in water (~2 mL) and precipitated two further times with EtOH (~30 mL). The pellets were dried under vacuum for 2 h. The dried product was stored at –20 °C. Crude yield: 0.26 g.

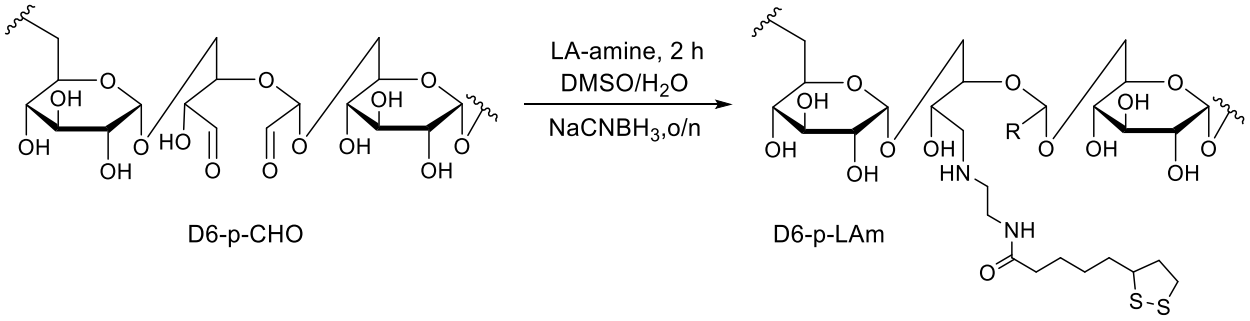

Scheme S8.

Pendant API-modified Dextran (D6-p-API)

Pendant API-modified dextran was synthesized as shown in Scheme S9. D6-p-CHO (1.0 g, 167 μmol of dextran, maximum 1.66 mmol aldehyde) was added to a 100 mL round bottom flask and dissolved in water (20 mL). Neat API (239 μL, 2 mmol) was added and the solution was mixed at room temperature for 2 h. Next, an aliquot of sodium cyanoborohydride (*aq*) (0.5 mL, 258 mg/mL in water, 2 mmol) was added to the reaction, which was then left to mix overnight at room temperature. The final reaction mixture was pipetted into ethanol (30 mL) to precipitate the dextran, which was then pelleted via centrifugation at 3000 rcf for 5 min. The supernatant was removed, and the pellet was redissolved in water (10 mL), and precipitated again with ethanol (30 mL), followed by centrifugation to collect the pellet of API-modified dextran (D6-p-API). The pellet was dried under vacuum to yield an off-white powder. Crude yield: 0.86 g.

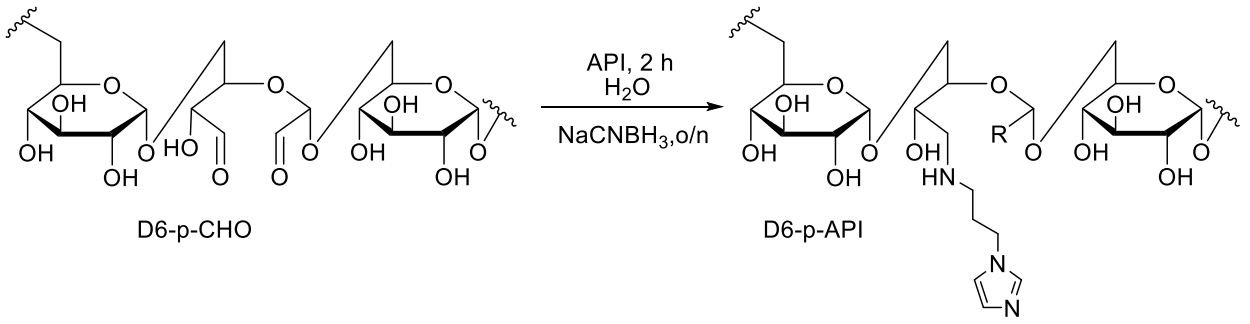

Scheme S9.

Characterization of Modified Dextran. After a modified dextran had been prepared, it was characterized using a range of methods.

^{1}H NMR

Dextran samples were prepared in deuterium oxide (D_2O) at a concentration of ~10 mg/600 μL. For each sample, a minimum of 32 scans were performed (more typically 512 scans) with a delay time of 4 s.

FTIR

ATR-FTIR measurements were made on powder samples deposited directly on the ATR crystal. Data were averaged over 8 scans.

Ninhydrin Tests

Ninhydrin tests were done to check for the presence of primary amine groups. Dextran samples (~0.8 μmol) were dissolved in water (100 μL) in microcentrifuge tubes before a ninhydrin solution (1% w/v ninhydrin in water, 100 μL) was added. The mixtures were briefly vortexed before incubating at 90 °C for 10 min. The microcentrifuge tubes were then imaged under ambient light using a smartphone camera.

TNBS Assay

TNBS assays were done to quantitate the number of amine groups per dextran. Standard solutions of ethanolamine with concentrations between 1–40 μg/mL were prepared by dilution of neat ethanolamine in bicarbonate buffer (100 mM, pH 9.28, denoted as the reaction buffer for this assay). The samples were prepared at concentrations of ~10 mg/mL for D10 samples and ~5 mg/mL for D6 samples. A 0.1% w/v solution of TNBS in reaction buffer was prepared by diluting a stock 1% w/v TNBS solution prepared in methanol. Aliquots of each sample or standard (80 μL) were transferred into a 96-well clear UV plate in triplicate. To each of these wells, 0.1% w/v TNBS (40 μL) was added. The well-plate was shaken for 10 s to mix the solutions before incubation at room temperature. Absorbance measurements at 420 nm were acquired 3 min after the addition of TNBS. A calibration plot of the absorbance at 420 nm versus

the ethanolamine concentration was prepared and used to determine the number of amine groups in the dextran samples.

Ellman's Assay

Ellman's assays were done to determine the number of thiol groups per dextran. This assay was done in 0.1 M sodium phosphate buffer with 1 mM EDTA, pH 7.9 (reaction buffer). A solution of DTNB in reaction buffer was prepared at a concentration of 4 mg/mL. Unmodified dextran samples were used as controls to ensure that the ligands were purified from the excess TCEP. All samples were dissolved in water with concentrations between 10–20 mg/mL. An aliquot (500 μL) of each solution was mixed with a TCEP solution (100 mg/mL in water, 20 equiv of TCEP versus dextran). The solutions were mixed at room temperature for 15 min and the reduced ligands were precipitated with EtOH (900 μL). The samples were centrifuged for 5 min at ~17 000 rcf. The supernatants were removed and the collected ligands were redispersed in water (100 μL) before being precipitated with EtOH (500 μL) again. This process was repeated for a total of four precipitation and wash steps. After the final wash, the collected ligands were redissolved in reaction buffer (500 μL). Samples of HMDA and LA (both ~100 μM; no reduction of LA) were tested as negative controls, and samples of GSH (~100 μM) were tested as positive controls.

An aliquot (20 μL) of each sample was diluted with reaction buffer (200 μL). In a 96-well plate, aliquots of the DTNB solution (3.2 μL) were added. To these wells, the dextran ligands were added (172 μL) in triplicate. The plate was shaken for 10 s then incubated at room temperature in the dark for 15 min. The absorbance was measured at 412 nm, where the molar absorption coefficient of the colored product is 14 150 M^{-1} cm^{-1}.[7,8] The concentration of sulfhydryls was then calculated using the Beer-Lambert Law, accounting for the dilution of the ligands. It was assumed that both sulfhydryls present in DHLA react with DTNB, as shown elsewhere.[9–11]

Anthrone Assay

Dextran concentrations were determined via an anthrone assay. A stock solution of dextran from *Leuconostoc spp.* (~6 kDa) in water was prepared (~2 mg/mL). This solution was used to prepare dextran standards ranging from 0–400 μg/mL. The ligand samples used in the previous TNBS

and Ellman's assays were diluted with water to an expected concentration of ~100 μg/mL. An anthrone solution was prepared in concentrated sulfuric acid (2 mg/mL). Aliquots of the dextran standards and samples (125 μL) were added to microcentrifuge tubes. Anthrone solution (375 μL) was then added to each of the microcentrifuge tubes. The tubes were carefully inverted and then cooled at 4 °C for 10 min. The tubes were inverted again to ensure complete mixing before incubation at ~80 °C for 45 min. The tubes were again cooled at 4 °C for 10 min. Aliquots of each of the solutions (100 μL) were transferred into a 96-well plate in quadruplicate. The absorbance was measured at 630 nm. A calibration curve of absorbance at 630 nm versus dextran concentration (μg/mL) was prepared and used to determine the quantity of dextran in each of the ligand samples.

Determining the Percent Functionalization of Dextran Ligands

The quantities of amine groups, thiol groups, and dextran in dextran ligand samples were determined using the TNBS, Ellman's, and anthrone assays described above. The percentage of functionalization was calculated via Eqn. S1, where [NH_2] was the concentration of amines determined via a TNBS assay, [SH] was the concentration of sulfhydryl groups determined via Ellman's assay, and [Dex] was the concentration of dextran determined by an anthrone assay. Assuming that both of the thiols present in DHLA reacted with the Ellman's reagent,[9–11] the percent DHLA per dextran was calculated by dividing the percent thiol per dextran by two.

$$\text{amine or thiols per dextran chain} = \frac{[NH_2] \text{ or } [SH]}{[Dex]} \times 100\% \qquad \text{(S1)}$$

Ligand Exchange Protocols. GSH-coated QDs were prepared following a previously published procedure.[12] Detailed procedures for the other ligands are described below.

Histidine (His)-QDs

His-QDs were prepared via modification of the GSH ligand exchange procedure.[12] Histidine (~200 mg, 1.3 mmol) was dissolved in 800 μL of TMAH in methanol in a microcentrifuge tube. An aliquot of a QD stock solution (48.5 μL, 206 μM, 10 nmol) was diluted to ~2 mL with chloroform in a glass vial. The histidine solution was added to the QDs, and the mixture was

vortexed and left to stand for 10 min. Borate buffer + salt (500 μL, 50 mM, 250 mM NaCl, pH 9.2) was added and the mixture was vortexed and the phases were left to separate. The QDs transferred to the aqueous phase, which was then transferred into two microcentrifuge tubes. EtOH was added to the point of turbidity and the samples were centrifuged to form pellets of QDs. The pellets were redispersed in borate buffer + salt and two further precipitation and wash cycles were performed. After the final wash, the QDs were redispersed in borate buffer without salt (50 mM, pH 9.2) and stored at 4 °C.

An alternative method was also used for some experiments and was adapted from previously published methods.[13,14] Histidine (~1.0 mg, 6.4 μmol) was dissolved in NaOH (*aq*) (0.2 M, 100 μL) mixed with methanol (200 μL) in a microcentrifuge tube. In a separate microcentrifuge tube, an aliquot of hydrophobic QDs (50 μL, ~25 μM, 1.25 nmol) was diluted with chloroform (100 μL). The solutions were combined and vortex mixed for 2 min. Further chloroform (200 μL) was added and the aqueous and organic phases were left to separate. The QDs transferred readily to the aqueous phase. The aqueous layer was then transferred to a clean microcentrifuge tube before being centrifuged for 1–2 min at 2000 rcf to pellet the QDs. The supernatant was removed and the QDs were redispersed in water (500 μL) and stored at 4 °C.

Dihydrolipoic acid (DHLA)-QDs

LA (2.1 mg, 10 μmol) was dissolved in 20 μL of DMSO in a microcentrifuge tube. TCEP-HCl (3.8 mg, 13 μmol) was dissolved in 100 μL of UPH_2O. The TCEP solution was added to the LA solution in the microcentrifuge tube and the solution turned cloudy but became clear upon vortexing. Bicarbonate buffer (100 μL, 100 mM, pH 9.33) was added to the mixture. An aliquot of His-QDs (55 μL, 9.1 μM, 0.50 nmol) was diluted with bicarbonate buffer (345 μL, 100 mM, pH 9.3) in a microcentrifuge tube. The reduced LA solution was added dropwise to the QDs before bicarbonate buffer (100 μL) was added. The mixture was incubated at 60 °C for 3 h. The DHLA-QDs were collected via spin filtration (30 kDa MWCO filter, EMD Millipore, Burlington, MA) and washed three times with bicarbonate buffer (300 μL). After the final wash, the QDs were transferred to a clean microcentrifuge tube and diluted with bicarbonate buffer so that the total volume was ~300 μL and stored at 4 °C.

(D-t-DHLA)-QDs

D6-t-LA (L) (64 mg, 10 μmol) was dissolved in water (400 μL) in a microcentrifuge tube. TCEP-HCl (38 mg, 0.13 mmol) was dissolved in water (200 μL) and added to the dextran solution. The solution was mixed at room temperature for 15 min, then split into two portions and precipitated with EtOH. The reduced dextran-DHLA was collected via centrifugation. The supernatant was withdrawn and discarded and the remaining translucent, viscous liquid/gel was redissolved in UPH_2O (200 μL total). The portions were recombined in a clean microcentrifuge tube and bicarbonate buffer (600 μL, 100 mM, pH 9.33) and an aliquot of His-QDs (55 μL, 9.1 μM, 0.50 nmol) were added. The mixture was incubated at 60 °C for 3 h. The dextran-coated QDs (Dex-QDs) were collected via spin filtration (30 kDa MWCO filter) and washed three times with bicarbonate buffer (300 μL, 100 mM, pH 9.3). After the final wash, the QDs were transferred to a clean microcentrifuge tube, diluted with bicarbonate buffer (100 mM, pH 9.3) to a total volume of ~300 μL, and stored at 4 °C in the dark.

An analogous procedure was applied with D10-t-LA, a mixture of D6-t-LA (L) and D10-t-LA (95% D6-t-LA (L) and 5% D10-t-LA by moles) and D6-t-LA (M). The masses were adjusted so that approximately the same molar quantity of ligand was used in each case.

(D6-p-X)-QDs where X = DHLA, DHLAm, or API

D6-p-LAm or D6-p-LA (13 mg or 15 mg, respectively; ~2 μmol of dextran) was dissolved in water (400 μL). TCEP-HCl (37 mg, 0.13 mmol) was dissolved in water (200 μL) and added to the dextran solution. Subsequent preparation and work-up of the D6-p-DHLA or D6-p-DHLAm QDs was analogous to that for the (D-t-DHLA)-QDs.

Dextran-API (14 mg, ~2 μmol of dextran) was dissolved in water (200 μL). Bicarbonate buffer (600 μL, 100 mM, pH 9.28) was added with an aliquot of His-QDs (55 μL, 9.1 μM, 0.50 nmol) and the mixture was incubated at 60 °C for 3 h. The work-up procedure was analogous to that for the (D-t-DHLA)-QDs.

Ligand Exchange Control Experiments

Ligand exchange procedures were performed using unmodified dextran or the amine-modified intermediates in the same manner as the method used for (D-t-DHLA)-QDs, except that no TCEP reduction step was performed.

Functional Tests of Dex-QDs. Dextran-functionalized QDs were characterized via different tests that confirmed modification of the QD surface with dextran.

FTIR

ATR-FTIR measurements were performed on QD samples. Aliquots (30 μL, 1–2 μM) of X-QD600 (X = His, D10-t-DHLA, D6-t-DHLA (L), D6-p-DHLA, D6-p-API and D6-p-DHLAm) and X-QD645 (X = His and D10-t-DHLA) were precipitated in EtOH (100 μL). The samples were centrifuged for 90 s at ~17 000 rcf. The supernatant was removed and DCM was added (30 μL). The pellet of QDs was transferred onto the ATR crystal and allowed to dry before measurements were obtained.

Anthrone Assay with QDs

A stock solution of dextran from *Leuconostoc spp.* (~6 kDa) in water was prepared (~2 mg/mL). This solution was used to prepare dextran standards ranging from 0–300 μg/mL. X-QD600 samples (X = DHLA, D10-t-DHLA, D6-t-DHLA (L), D6-p-API, D6-p-DHLA, and D6-p-DHLAm) were diluted 400-fold in water to concentrations of ~3.2–4.4 nM. An anthrone solution was prepared in concentrated sulfuric acid (2 mg/mL). Aliquots of the dextran standards and QD samples (200 μL) were added to microcentrifuge tubes. The samples were prepared in duplicate and the anthrone assay was done as described earlier (pg. S-16). The number of dextran chains per QD was estimated from the quantity of dextran determined for each of the QD samples.

Tests with ConA Protein

Phosphate buffered saline (1× PBS; pH 7.2, 1.54 mM KH_2PO_4, 2.71 mM Na_2HPO_4, 155 mM NaCl) was supplemented with $CaCl_2$ and $MnCl_2$ so that the metal ions were at a final concentration of 1.0 mM. Stock solutions of ConA (10 μM) and glucose (200 mM) were prepared in the supplemented PBS buffer. Aliquots (1 μL, 1 μM) of X-QD600 (X = D6-t-DHLA,

D6-p-DHLAm, D6-p-DHLA, D6-p-API, and DHLA) were prepared in supplemented PBS buffer (19 μL), in buffer (9 μL) with an aliquot of ConA (10 μL of stock), and in buffer (4 μL) with aliquots of both ConA (10 μL of stock) and glucose (5 μL of stock). These samples were left at room temperature for 30 min before splitting the reaction mixtures into two portions. One portion was centrifuged for 5 min at 4800 rcf and subsequently imaged under UV illumination. The other portion was mixed with 50% v/v glycerol (*aq*, 2.5 μL), then loaded into a 0.5% w/v agarose gel prepared in 1× TBE buffer. The gel was run at a field strength of ~6.7 V cm^{-1} for 30 min before imaging under UV illumination.

Tests with ConA, BSA, and lysozyme

All samples were prepared to a final concentration of 50 nM (D10-t-DHLA)-QD600. Briefly, the QDs were incubated with 100 equivalents BSA, lysozyme, or ConA which were all prepared in 1× PBS supplemented with 1 mM $CaCl_2$ and $MnCl_2$. The concentrations of the various proteins were 5 μM in all the samples prepared. A control sample was prepared with no protein added. The samples were spiked with glycerol to a final concentration of 2% (v/v). An agarose gel was run for 30 min at ~6.7 V cm^{-1} in 1× TBE buffer (100 mM, pH 8.3) and imaged under UV illumination.

Tests with ConA-Sepharose

Specific binding and elution of dextran-functionalized QDs were also evaluated with ConA-sepharose (an affinity chromatography resin that binds α-D-mannopyranosyl, α-D-glucopyranosyl, and other sterically similar groups). Elution of specifically bound species is achieved by competition with D-glucose.

In a first experiment, an aliquot of ConA-sepharose (500 μL) was washed twice with Tris buffer (pH 7.7, 0.5 M NaCl, containing 1 mM $MgCl_2$, 1 mM $MnCl_2$, and 1 mM $CaCl_2$) by mixing the resin with 1 mL of buffer, followed by centrifugation and removal of the supernatant after each wash. Samples of (D3.5-t-DHLA)-QD630 and His-QD630 (20 μL, 8 pmol) were prepared in the aforementioned Tris buffer plus 0.1% w/v BSA. QD aliquots were added to the resin in two separate microcentrifuge tubes, the samples mixed for 15 min on a rotary mixer, and centrifuged to pellet the resin. The supernatant of each sample was removed and its PL spectrum was

measured. An elution procedure that included a wash step with a 1.5% w/v BSA solution (400 μL), centrifugation, and collection and measurement of the supernatant was then done. An analogous elution procedure with 0.5 M glucose in Tris buffer (500 μL) was subsequently done.

A second experiment was done using DHLA-QDs as a reference. An aliquot of ConA-sepharose resin (500 μL) was washed five times with Tris buffer (pH 7.7, 0.5 M NaCl, containing 1 mM $MgCl_2$, 1 mM $MnCl_2$, and 1 mM $CaCl_2$). After washing, 20 μL aliquots of (D6-t-DHLA)-QD645 and (DHLA)-QD645 (110 pmol) were prepared in 80 μL of the aforementioned buffer plus 0.6% w/v BSA. The QD samples were added to the resin in two separate microcentrifuge tubes, the samples were mixed for 20 min on a rotary mixer, and centrifuged to pellet the resin. The supernatant for each sample was removed and its PL spectrum was measured. An elution step using 500 μL of a 0.5 M D-glucose in Tris buffer solution was then done.

Optical Characterization. UV-visible absorbance spectra of the aqueous QDs were collected between 400–800 nm with a path length of 1.0 cm.

PL emission spectra were measured between 450–800 nm with an emission monochromator bandwidth of 5 nm and an excitation wavelength of 400 nm and bandwidth of 5 nm. Quantum yield (Φ) measurements were done with QD600 samples using fluorescein in borate buffer (50 mM, pH 9.2) as a reference (Φ = 0.93).[15] PL emission spectra for various dilutions of fluorescein and QD samples were measured between 460–700 nm using 450 nm excitation. The PL spectra were integrated between 465–700 nm and plotted against absorbance at 450 nm. Quantum yield values were calculated from the slope of the plots and Eqn. S2, where Φ is a quantum yield of either the QDs (X) or the fluorescein standard (ST), and η is the refractive index of the solvent. All measurements were made in aqueous solution, such that the refractive index correction was unnecessary.

$$\Phi_X = \Phi_{ST}\left(\frac{\text{Slope}_X}{\text{Slope}_{ST}}\right)\left(\frac{\eta_X^2}{\eta_{ST}^2}\right) \qquad \text{(S2)}$$

Size Characterization. QDs were analyzed via DLS. Measurements were performed on 60 μL aliquots of QDs in bicarbonate or borate buffer. The modal value for the number-weighted plots were averaged across at least three replicate measurements.

For NTA measurements, the QD samples were diluted to less than 10 pM in a glycerol/water mixture (40% v/v glycerol) and were analyzed by fluorescence mode NTA. Measurements were made at 25 °C and the viscosity was set to 4.05 cP. The particle size data was fit with a lognormal distribution and the modal values were averaged across three replicate measurements. Control measurements were also done on 50 nm citrate-coated gold nanoparticles (AuNPs) as reference materials. The AuNPs were diluted in water or glycerol/water mixture (40% v/v glycerol) and analyzed by scattering mode NTA. The data for the AuNPs was fit with a lognormal distribution and the mean values were averaged across three replicate measurements. The relative size difference between the citrate-coated AuNPs in water versus glycerol/water was used to derive a correction factor. This value was then applied to the values for the QD sizes to account for the smaller solvodynamic size in 40% v/v glycerol (*aq*).

Preparation of Scale Illustrations of Dex-QDs. Scale illustrations (main text, Figure 1B–C) were prepared to represent QD600 coated with different modified dextran ligands (D10-t-DHLA, D6-t-DHLA and D6-p-DHLA) and TAC. The QD is represented as a sphere with a diameter of 9.8 nm (from TEM data). The translucent blue spheres represent the diameters of Dex-QDs as measured by DLS (see Table 1 in main text). Glucose oligomers and lipoic acid moieties were generated in Avogadro, Version 1.2.0[16] and were attached to dextran in Chimera, Version 1.13.[17] The degree of 1,3 branching in each strand was estimated based on the relative integrations of the anomeric signals in the ^{1}H NMR spectra of the 6 kDa and 10 kDa dextran, as described previously.[18,19] Pendant ligands are shown with 2–3 pendant lipoic acid moieties randomly distributed along the length of the dextran. Plausible conformations of dextran were generated by permuting the dihedral angles joining each glucose monomer until the ligand length predicted by the DLS data was achieved. A TAC was approximated and illustrated using four copies of a mouse monoclonal antibody (PDB: 1IGY[20]). Two of these copies were cleaved on the C-terminal side of Phe254 to represent the pepsin cleavage of the bridging antibodies to their F(ab')$_2$ fragments, as described previously.[21] The goal of these illustrations is to provide a sense of scale.

The models are not energy-minimized structures. The TAC illustration is based on published studies[21] and not information from the manufacturer.

Electrophoretic Mobility

Agarose Gel Electrophoresis

Unless otherwise stated, agarose gels (1.0% w/v) were prepared in 1× TBE buffer (pH 8.3) and QD samples (~1 pmol) were diluted with bicarbonate buffer (100 mM, pH 9.3) and spiked with 50% v/v glycerol solution (1–2 μL, final glycerol content 10% v/v for the sample). The gels were run for ~30 min at ~6.7 V cm^{-1} and imaged under UV illumination.

Capillary Electrophoresis

For CE experiments, the capillary was preconditioned by rinsing in sequence with methanol, 0.1 M NaOH (*aq*), water, and borate buffer (20 mM, pH 9.3) for 5 min each. All samples were prepared in borate buffer with added fluorescein (100 μM) as an internal standard. QD600 samples were 200 nM. Rhodamine B (100 μM) was used as a reference neutral analyte. The capillary was rinsed with borate buffer (20 mM, pH 9.3) for 4 min prior to each injection (5 s injection time, 50 mbar injection pressure). Borate buffer (20 mM, pH 9.3) was used for the sample runs. QDs were hydrodynamically injected (see pg. S-8) at the anodic side of the capillary and traveled towards the cathode with the electroosmotic flow. Following each sample run, the capillary was post-conditioned by successive rinses with 0.1 M NaOH and water for 3 min each. The pressure was 1 bar during rinses and the sample runs. The temperature was maintained at 20 °C. Data were recorded at multiple wavelengths, but the electropherograms were plotted for the signal at 260 nm. All CE runs were performed in triplicate.

Colloidal Stability. For colloidal stability tests as a function of pH, 1.5 μM solutions of QDs were prepared in bicarbonate buffer (100 mM, pH 9.3). A 10 μL aliquot of each sample was then diluted with 90 μL of phosphate/citrate buffers (100–200 mM, pH 3.0, 4.1, 5.1, 6.0, 7.0, 8.1). Colloidal stability was also tested in high-ionic strength bicarbonate buffer (100 mM, pH 9.3, 1.0 M NaCl). Samples were stored at room temperature, in the dark, and monitored over time via

imaging with a smartphone camera under long-wave UV illumination. Before imaging, the samples were centrifuged at 2000 rcf for a few seconds.

Cell Culture and Fixation

Cell Culture

SK-BR3 cells (ATCC HTB-30, Manassas, VA), a human breast cancer cell line, were cultured in a humidified incubator with 95% air/5% CO_2 at 37 °C. The culture medium was McCoy's 5A (GE Healthcare, Chicago, IL) supplemented with 10% v/v fetal bovine serum and 1× antibiotic and antimycotic (ThermoFisher, Waltham, MA). Cells were cultured in T25 flasks and subcultured every 5–7 days.

A549 cells (ATCC CCL-185), a human lung carcinoma cell line, that were used for non-specific binding studies were cultured analogously to the SK-BR3 cells. A549 cells used for microinjection experiments were cultured under the same conditions, except that the culture medium used was Ham's F-12K media (Gibco, Grand Islands, NY) supplemented with 10% v/v fetal bovine serum and 1× antibiotic and antimycotic.

MDA-MB-231 cells (ATCC HTB-26), a human epithelial breast cancer cell line, were cultured analogously to the SK-BR3 cells, except that the culture medium used was DMEM (Sigma Aldrich) supplemented with 10% v/v fetal bovine serum, 1× antibiotic and antimycotic (ThermoFisher), 2 mM L-glutamine (Gibco, 25030081), and 0.1 mM MEM non-essential amino acids (Gibco, 11140-050).

Fixing SK-BR3 Cells

A ~1×10^6 cell suspension of fixed SK-BR3 cells was prepared by pelleting freshly trypsinized SK-BR3 cells via centrifugation at 55 rcf for 5 min. The supernatant was removed, and the pellet was resuspended in 2 mL of 1× PBS buffer (Gibco Life Technologies). The cells were fixed by adding 2 mL of 4% w/v paraformaldehyde (prepared in 1× PBS) and gently mixing via pipette. The sample was incubated at room temperature for 5–10 min before pelleting via centrifugation

at 55 rcf for 5 min. The supernatant was discarded, and the pellet was resuspended in 4 mL of 1× PBS buffer.

Non-Specific Binding Experiments. Non-specific binding with proteins and cells was compared between dextran-functionalized QDs and small molecule-functionalized QDs (His, DHLA, or GSH ligands).

Non-Specific Binding Studies with Proteins via Gel Electrophoresis

Agarose gel electrophoresis was used to evaluate protein adsorption on X-QDs, where X = D10-t-DHLA, D6-p-DHLA, D6-p-API, GSH, DHLA, or His. The proteins or protein matrices tested were bovine serum albumin (BSA), lysozyme, skim milk powder (primarily casein), and bovine plasma. Stock solutions of 10 mg/mL protein (not including plasma) were prepared in bicarbonate buffer (pH 9.2). Lyophilized bovine plasma was reconstituted in 10 mL sterile water as per the manufacturers' instructions. Solutions containing X-QD600 or X-QD645 (2 pmol) and 1.0, 5.0, and 9.5 mg/mL (or 10%, 50%, and 95% v/v) of the protein (or plasma) stock solutions were prepared at a final volume of 20 μL. Samples were incubated at room temperature for 3.5 h. The samples were spiked with 5 μL of 50% v/v glycerol (*aq*) and loaded into the wells of a 1.0% w/v agarose gel prepared with 1× TBE buffer. The gel was run at a field strength of ~6.7 V cm^{-1} for ~40 min, then imaged under UV illumination.

Non-Specific Binding Studies with Cells

MDA-MB-231 and A549 cells were grown in tissue-culture treated, cover-glass bottom, 8-well chamber slides (Eppendorf, Hamburg, Germany). Each well was seeded with ~30 000 cells. The cells were grown until confluency (between 72–96 h) before proceeding with non-specific binding experiments.

Once cells were confluent, the media was removed and the cells were washed with HEPES-KRH buffer (300 μL; pH 7.2, 120 mM NaCl, 5 mM KCl, 2mM $CaCl_2$, 1 mM $MgCl_2$, 25 mM $NaHCO_3$, 5.5 mM HEPES, 1 mM D-glucose). X-QD600, where X = GSH, D6-t-DHLA (L), D10-t-DHLA, D6/10-t-DHLA, D6-t-DHLA (M), D6-p-DHLA, and D6-p-API, were prepared at a final concentration of 50 nM in HEPES-KRH buffer. (D6-p-DHLA and D6-p-API were prepared from

D6 (L).) The washed cells were incubated with the QD solutions for 30 min in a humidified incubator with 95% air/5% CO_2 at 37 °C. The QD solutions were removed, and the cells were washed twice with HEPES-KRH buffer (300 μL) to remove unbound QDs. The samples were then imaged in 300 μL HEPES-KRH buffer. The assays were performed in triplicate.

A quantitative assay was also performed with A549 and MDA-MB-231 cells to evaluate the non-specific binding of X-QD600, where X = GSH, D10-t-DHLA, D6-p-DHLA. Cells were seeded into a 96-well tissue culture-treated clear-bottom plate (ThermoFisher, Waltham, MA). The cell media was removed, and the cells were washed with HEPES-KRH buffer (100 μL). Solutions of QDs were prepared in HEPES-KRH buffer at concentrations of 10, 30, 50, 70 and 100 nM. Aliquots of the QD samples (90 μL) were added to the cells and the cells were incubated for 30 min in a humidified incubator with 95% air/5% CO_2 at 37 °C. The QDs were removed and the cells were washed twice with HEPES-KRH buffer (100 μL) before absorbance and PL emission spectra were collected on a plate reader. The assay was performed in duplicate.

Cellular Microinjection. Sterile cell culture dishes were pre-treated with fibronectin (5 μg/mL) in a humidified incubator with 95% air/5% CO_2 at 37 °C for > 6 h prior to seeding cells. Approximately 3×10^5 A549 cells were seeded into a pre-treated cell culture dish (35 mm dish diameter, 14 mm diameter glass bottom, 0.08–0.12 mm thick glass bottom; Matsunami Glass Ind., Ltd., Osaka, Japan). After transfer, the A549 cells were grown in supplemented McCoy's 5A media (no phenol red; Gibco) for ≥ 16 h. For some experiments, immediately prior to microinjection, the media was removed and the dish was filled with 1× PBS(++) buffer (0.90 mM $CaCl_2$, 0.49 mM $MgCl_2$, 2.67 mM KCl, 1.47 mM KH_2PO_4, 138 mM NaCl, 8.06 mM Na_2HPO_4). Microinjections were done with a 100–200 hPa injection pressure and 0.3–1.0 s injection times. Solutions of dextran-functionalized QDs (0.74 μM for (D10-t-DHLA)-QD600, 0.81 μM for (D6-p-DHLA)-QD600, 0.75 μM for (D6-p-API)-QD600, in HEPES buffer (200 mM, pH 7.2)) were filtered using a 0.22 μm-porous membrane syringe filter (Millex-GP, Merck Millipore Ltd., Tullagreen, Carrigtwohill, Co. Cork, Ireland), then centrifuged at ~17 000 rcf for 15 min prior to loading the supernatant into the microinjection needle. Brightfield and fluorescence images were acquired prior to injections and at various time intervals following the injections.

Cell Viability Assays. The potential cytotoxicity of (D10-t-DHLA)-QD600 was assessed using a 3-(4,5-dimethylthiazol-2-yl)-5-(3-carboxymethoxyphenyl)-2-(4-sulfophenyl)-2H-tetrazolium inner salt (MTS) assay kit (Abcam, Toronto, ON, Canada). A549 cells were seeded in a 96-well tissue culture-treated clear-bottom plate (ThermoFisher, Waltham, MA) at ~10 000 cells/well and grown overnight in a humidified incubator with 95% air/5% CO_2 at 37 °C. Cells were washed with HEPES-KRH buffer (100 μL) and incubated with QD solutions (10 pM–1 μM) for either 3 h or 24 h in a humidified incubator with 95% air/5% CO_2 at 37 °C. Following incubation, the QD solutions were removed and the cells were washed with HEPES-KRH buffer (100 μL). McCoy's 5A media without phenol red (90 μL) was then added to the cells, which were left to grow for 3 days in a humidified incubator with 95% air/5% CO_2 at 37 °C. After this proliferation period, MTS reagent solution (10 μL) was added to each well and the cells were incubated for 2 h in a humidified incubator with 95% air/5% CO_2 at 37 °C. The absorbance was measured at 490 nm (analytical wavelength) and 650 nm (for background subtraction). Cellular viabilities were reported as the percentage of the absorbance for negative control wells (non-treated cells). The assays were performed in triplicate.

Covalent Conjugation and pH Sensing

FITC-labeling of (D6-t-DHLA)-QDs

FITC-labeled (D6-t-DHLA)-QD600 were prepared by mixing an aliquot of QDs (7.5 μL, 1 μM) in bicarbonate buffer (0.1 M, pH 8.8) with a FITC solution (0.5 mg/mL, 7.5 μL) in DMSO. The reaction was left overnight at room temperature and the QDs were purified from unreacted FITC using a 10 kDa MWCO spin-filter (VWR International, Mississauga, ON, Canada). A negative control sample was prepared analogously, but used fluorescein (no reactive group) instead of FITC. The labeled QDs were diluted to a final concentration of ~0.5 μM in bicarbonate buffer.

Additional control samples were prepared with only FITC or fluorescein (no QDs) by mixing an aliquot (0.5 mg/mL in DMSO, 7.5 μL) with bicarbonate buffer (100 mM, pH 9, 7.5 μL). A control sample of (D6-t-DHLA)-QD600 was prepared by diluting an aliquot of QDs (7.5 μL, 1 μM) with bicarbonate buffer (100 mM, pH 9, 7.5 μL). Samples were loaded into a 1% w/v

agarose gel prepared in 1× TBE buffer, and run at a field strength of ~6.7 V cm^{-1} for 12 min. The gel was imaged under UV illumination.

pH Sensing

To prepare pH sensors, the above reaction was scaled up. (D6-t-DHLA)-QD600 were diluted to a final concentration of 1 μM in bicarbonate buffer (100 μL, 100 mM, pH 9) and mixed with FITC (0.5 mg/mL in DMSO, 100 μL). The sample was left overnight at room temperature, protected from light, with shaking. To separate labeled QDs from excess dye, the QDs were precipitated with absolute ethanol (400 μL). The labeled QDs were pelleted via centrifugation, and the supernatant (containing unreacted FITC) was removed. The QDs were resuspended in UPH_2O, and the precipitation and washing step was repeated once more. The QD pellet was dried under vacuum and then resuspended in UPH_2O (200 μL) at a final QD concentration of ~0.5 μM.

For pH sensing experiments, FITC-labeled QD samples (20 μL, 0.5 μM) were mixed with an equal volume (20 μL) of the following buffers: 100 mM MES buffers (pH 4.5 and 6.5), 100 mM sodium phosphate buffer (pH 7.0), 100 mM borate buffer (pH 8.5), and 100 mM bicarbonate buffers (pH 8.5, 9.1 and 10.5). The samples were transferred to a 96-well plate and PL emission spectra (475–800 nm, 2 nm step-size, 450 nm excitation wavelength) were measured.

Peptide Assembly and Proteolytic Activity Assays

Peptide Self-Assembly on QDs

Dextran-functionalized QD-peptide conjugates were prepared by mixing (D6-t-DHLA)-QD645 (20 pmol) with 5, 10, 20 and 30 equivalents of Alexa Fluor 680 (A680)-labeled peptides in borate buffer (20 mM, pH 8.5). The peptide sequence is given in Table S1 (entry 1). Labeling was done as described previously.[1] The samples were incubated at room temperature for 55 min and then transferred to a black, nonbinding 96-well plate (#3650; Corning, Corning, NY). PL emission was measured between 500–850 nm (2 nm step size, 5 nm bandwidth) using 450 nm excitation (to avoid direct excitation of the A680 dye). Peptide binding to the QD surface was confirmed using agarose gel electrophoresis. Aliquots (15 μL) from samples of the QD-peptide conjugates were spiked with 5 μL of 50% v/v glycerol (*aq*) and loaded into the wells of a 1.0%

w/v agarose gel prepared with 1× TBE buffer. The gel was run at a field strength of ~6.7 V cm^{-1} for 50 min, then imaged under UV illumination.

Analogous experiments were performed using the same peptide but labeled with Alexa Fluor 647 (A647) dye and X-QD600, where X = D10-t-DHLA, D6-p-DHLA, D6-p-DHLAm, and D6-p-API. The peptide sequence is given in Table S1 (entry 2). X-QDs (5 pmol) were incubated with 5, 10, 20 or 30 equivalents of A647 in borate buffer (50 mM, pH 9.2), with total reaction volumes of 20 μL, for 1 h at room temperature. The samples were then diluted with borate buffer (60 μL, 50 mM, pH 9.2) and their PL emission spectra measured between 450–800 nm (400 nm excitation to avoid direct excitation of the A647 dye). Aliquots (15 μL) from the samples of QD-peptide conjugates were spiked with 5 μL of 50% v/v glycerol (*aq*) and loaded into the wells of a 1.0% w/v agarose gel prepared with 1× TBE buffer. The gel was ~6.7 V cm^{-1} for 30 min, then imaged under UV illumination.

Table S1. Peptide sequences (written N-terminal to C-terminal).

1	--	[Ac]HHHHHHSPPPPPSGQGEGGNSDDDDKSGNGC*(A680)
2	--	[Ac]HHHHHHSPPPPPSGQGEGGNSDDDDKSGNGC*(A647)
3	nsLys	[Ac]HHHHHHGPPPPPGSDGNEGNL**K**GSGC*(A647)
4	nsArg	[Ac]HHHHHHGPPPPPGSDGNEGNL**R**GSGC*(A647)

The * indicates dye labeling at the side chain. [Ac] indicates N-terminal acetylation. Proteolysis occurs C-terminal to the bolded residue.

Proteolytic Activity Assays

To assemble peptide substrates to X-QDs, A647-labeled peptides (0.4 mM in pH 9.2 borate buffer, 400 pmol, 8 equivalents) were added to QDs (50 pmol, 5–12 μM in pH 9.2 bicarbonate buffer for X = modified dextran or pH 9.2 borate buffer for X = GSH). The peptide sequences are given in Table S1 (entries 3 and 4). The ligands tested were X = GSH, D6-t-DHLA, D10-t-DHLA, D6-p-DHLA, and D6-p-API. The solutions were mixed, left in the dark at room temperature overnight, and subsequently stored at 4 °C.

Assays were done in black polystyrene 96-well assay plates. For each sample, QD-peptide conjugates (3.0 pmol) were diluted to a final volume of 30 μL with 1× PBS buffer. Assays were

started by adding 30 µL of protease solution (at twice the desired final concentration of protease) in 1× PBS buffer to the QD-peptide conjugates. Negative control samples were QD-peptide conjugates (3.0 pmol) diluted to 60 µL with 1× PBS buffer (*i.e.* no added protease), and were prepared for each ligand tested. PL emission intensities at 605 nm (QD, 7 nm bandwidth) and 670 nm (A647, 7 nm bandwidth) were measured every minute for 90 min (405 nm excitation, 7 nm bandwidth) using a plate reader. As described previously,[22–24] normalized FRET-based reaction progress curves were calculated using Eqn. S3, where ρ(t) is the normalized PL emission ratio and $I_{670,x}$(t) and $I_{605,x}(t)$ are the PL emission intensities, as a function of time, t, at 670 nm and 605 nm, in the presence of x nM of protease. $I_{670,0}(t)$ and $I_{605,0}(t)$ refer to the PL intensities of the negative control sample at 670 nm and 605 nm.

$$\rho(t) = \frac{I_{670,x}(\mathrm{t})/I_{605,x}(t)}{I_{670,0}(\mathrm{t})/I_{605,0}(t)} \qquad \text{(S3)}$$

Conjugation with Tetrameric Antibody Complexes (TAC) and Applications

Preparation of TAC Anti-Target Immunocomplexes

Bifunctional anti-target TACs, which consisted of an anti-dextran antibody on one end and an anti-target (*e.g.* EPO, HER2) binding antibody on the other end were prepared according to the instructions of an EasySep™ Human "Do-It-Yourself" Positive Selection Kit II immunomagnetic positive selection cell isolation kit (STEMCELL Technologies, Vancouver BC, Canada). The anti-target antibody was either a mouse monoclonal anti-human EPO antibody (EPO-16, clone 16F1H11, mouse monoclonal antibody to human erythropoietin; STEMCELL Technologies) or a mouse anti-human HER2 antibody (clone HRB2/282; Novus Biologicals, Burlington, ON, Canada). The desired anti-target antibody (15 µg) was mixed with kit *Component A* (100 µL) and kit *Component B* (100 µL) solutions, in sequence. The sample was incubated overnight at 37 °C then diluted with 1× PBS buffer (up to 1 mL). TACs were stored at 4 °C until needed.

Binding of TAC to Dextran-Functionalized QDs

Agarose gel electrophoresis was used to confirm anti-dextran antibody and TAC binding to (D6-t-DHLA)-QD645. For confirmation of antibody binding, (D6-t-DHLA)-QD645 (1 μL, 1.2 pmol) were mixed with 20 μL of *Buffer B* and 10 μL of *Component A* from an EasySep™ Do-It-Yourself Selection Kit (STEMCELL Technologies). The solution was incubated for 1.5 h at room temperature before being analyzed via agarose gel electrophoresis (1% w/v agarose gel, ~6.7 V cm^{-1} for 30 min). The gel was imaged under UV illumination. A control sample of (D6-t-DHLA)-QD645 was run for comparison.

For confirmation of TAC binding, samples were prepared by overnight incubation of (D6-t-DHLA)-QD645 (1.5 μL, 1.5 pmol) with TAC anti-EPO complexes (5 μL, 30 pmol, 20:1 TAC:QD ratio) at 37 °C in 10 μL of *Buffer B* (EPO ELISA kit, STEMCELL Technologies). The samples were cooled to room temperature, and spiked with 3.5 μL of 50% v/v glycerol (*aq*) for a total sample volume of 20 μL. The sample was then loaded into the wells of a 1% w/v agarose gel prepared in 1× TBE buffer and run at a field strength of ~6.7 V cm^{-1} for 45 min. The gel was imaged under UV illumination. A control sample of (D6-t-DHLA)-QD645 was run for comparison.

As another confirmation of TAC binding, samples were prepared by incubating (D10-t-DHLA)-QD645 (2 μL, 0.3 pmol) with TAC anti-EPO complexes in varying ratios (0–6:1 TAC:QD). The samples were incubated in bicarbonate buffer (50 mM, pH = 9.2) for 3.5 hrs, and spiked with 5 μL of 50% v/v glycerol (*aq*) for a total sample volume of 25 μL. The sample was then loaded into the wells of a 1% w/v agarose gel prepared in 1× TBE buffer and run at ~6.7 V cm^{-1} for 45 min. The gel was imaged under UV illumination. A control sample of (D10-t-DHLA)-QD645 was run for comparison.

EPO Immunoassay

PL emission-based sandwich immunoassays for the detection of human EPO were done by modification of a commercial kit (STEMCELL Technologies). The kit included a 96-well microtiter plate for immunoaffinity isolation (wells coated with a high-affinity monoclonal anti-EPO antibody) and buffer components. Stock solutions of conjugates of (D10-t-DHLA)-QD645

and TAC anti-EPO were prepared immediately before use. QD-TAC conjugates were prepared in 1.7 mL microcentrifuge tubes by mixing (D10-t-DHLA)-QD645 (2.5 pmol) with TAC anti-EPO (ratio of 7.3:1 TAC:QD) in *Buffer B* from the ELISA kit. The solutions stood at room temperature for 90 min.

For the immunoassay, *Buffer A* (25 µL) from the ELISA kit was added to each well, followed by a 50 mU/mL human EPO standard solution (100 µL, from ELISA kit). The QD-TAC conjugate was then added to the wells and samples were incubated overnight at room temperature. After incubation, the wells were washed five times with *Wash Buffer* (100 µL) from the ELISA kit. Either full PL emission spectra (490–750 nm) or single-point PL intensities at 670 nm were measured with a plate reader (both with an excitation wavelength of 450 nm). EPO-positive and EPO-negative samples were measured alongside three control samples: a blank well, QD with no TAC but with EPO, and QD only (no TAC, no EPO). Analogous experiments were also done with (D10-t-DHLA)-QD600 conjugated with TAC anti-EPO and 5000 mU of EPO added (rhEPO from STEMCELL Technologies).

SK-BR3 Immunolabeling and Imaging

A suspension of fixed SK-BR3 cells (in 1× PBS) were immunolabeled with TAC anti-HER2 and (D6-p-DHLAm)-QD600. SK-BR3 cells (10 µL, 0.5×10^6 cells/mL) were pipetted into a 1.7 mL Eppendorf tube, followed by 12.3 µL of TAC anti-HER2 (97 nM, or 15 µg/mL, 1.2 pmol), and, lastly, (D6-p-DHLAm)-QD600 (0.5 pmol in water). A control sample, which did not include TAC anti-HER2 complex, was prepared as above but was spiked with 12.3 µL of 1× PBS buffer instead. The samples were mixed via pipette and incubated at room temperature, protected from light, for 30 min. The samples were pelleted via centrifugation at 55 rcf for 5 min. The supernatant, which contained excess/unbound QDs, was removed via pipette. The cells were then resuspended in 20 µL of 1× PBS. For imaging, the samples were drop cast on a microscope slide and a cover slip was applied. The samples were inverted and imaged through the cover slip.

Supplementary Results and Discussion

Ligand Characterization. ^{1}H NMR spectra were collected for the starting materials and the modified dextrans (Figures S1–S4). There are residual solvent peaks in many of the spectra.

For reducing-end modified dextran, the appearance of new peaks in the alkyl region indicated that modification with HMDA and, subsequently, LA were successful. The ratio between the integrals for the anomeric proton of dextran and those for the newly introduced moieties suggested that the modification occurred with modest yields. (This result was confirmed by colorimetric assays, *vide infra*.)

For pendantly-modified dextran, the appearance of small peaks in the aldehyde region was consistent with successful partial oxidation along the dextran chains using sodium (meta)periodate. Small peaks in the region of 5–6 ppm were also observed and may correspond to hemi-acetal formation of the oxidized dextran.[25] These peaks were no longer visible after the reductive amination steps to pendantly modify the dextran, and new peaks corresponding to the LA derivatives or API were observed, indicating that these reactions were successful.

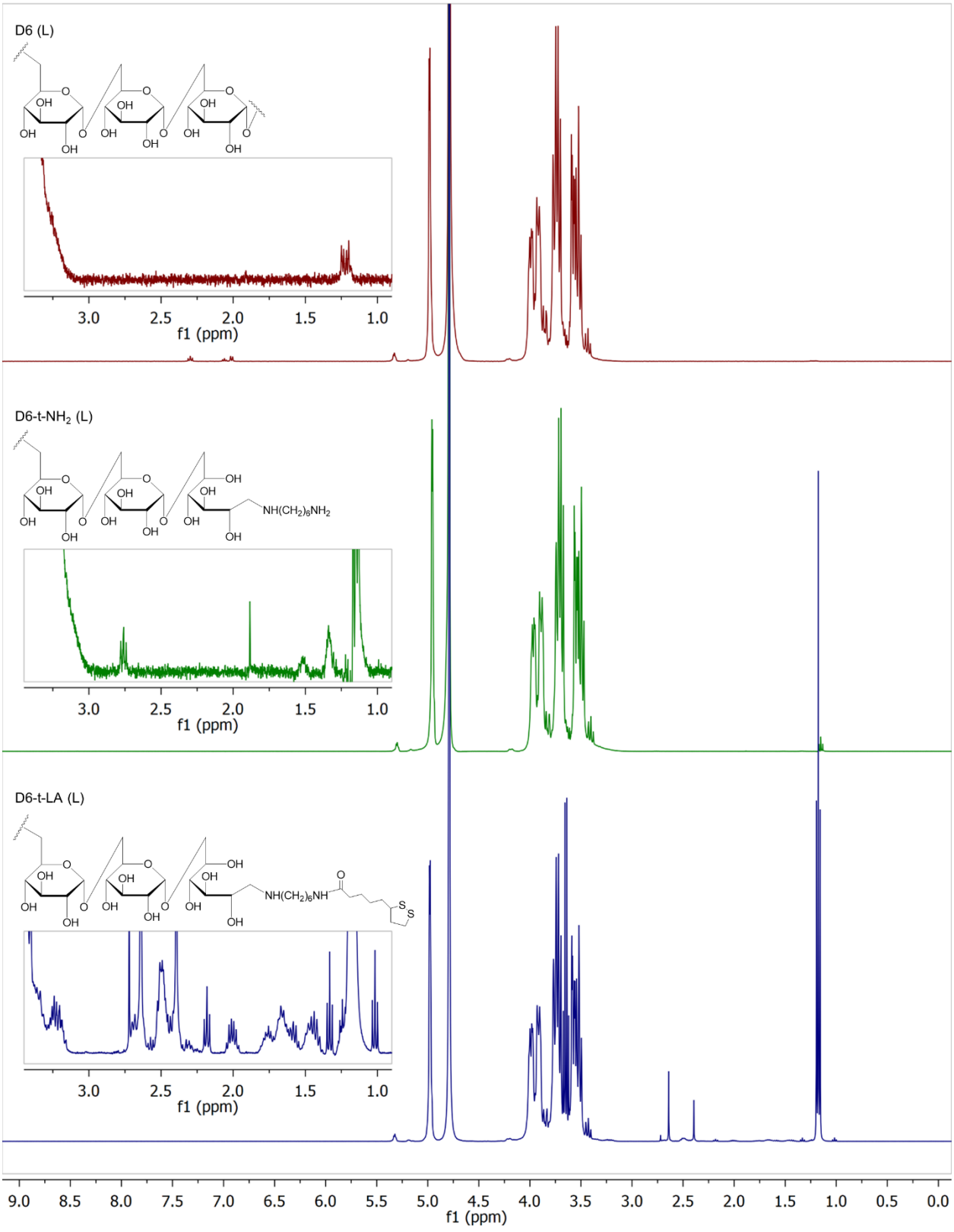

Figure S1. Stacked ^{1}H NMR spectra for D6 (L) (red), D6-t-NH_2 (L) (green), and D6-t-LA (L) (blue). The inset zooms in on 0.9–3.45 ppm.

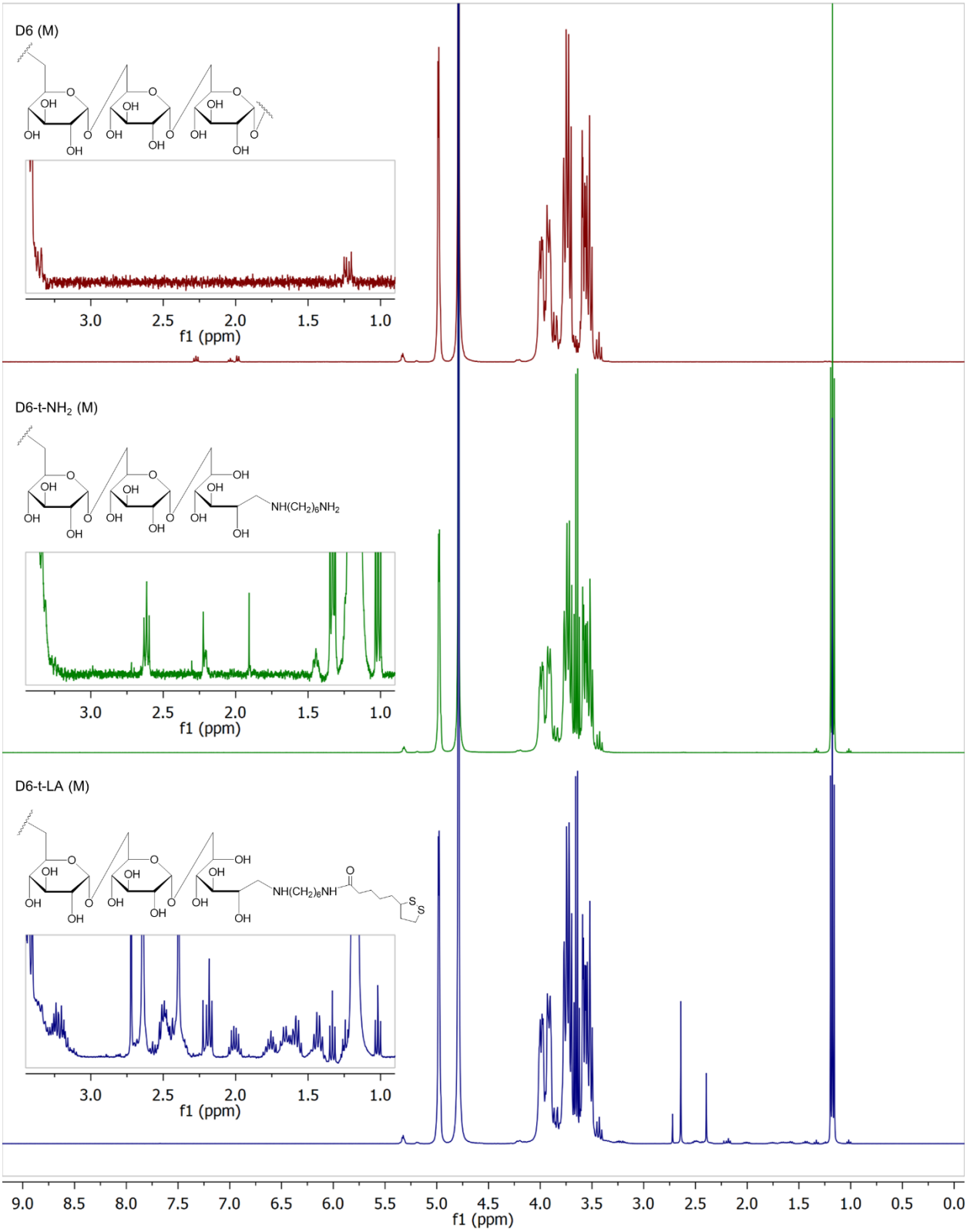

Figure S2. Stacked ^{1}H NMR spectra for D6 (M) (red), D6-t-NH_2 (M) (green), and D6-t-LA (M) (blue). The inset zooms in on 0.9–3.45 ppm.

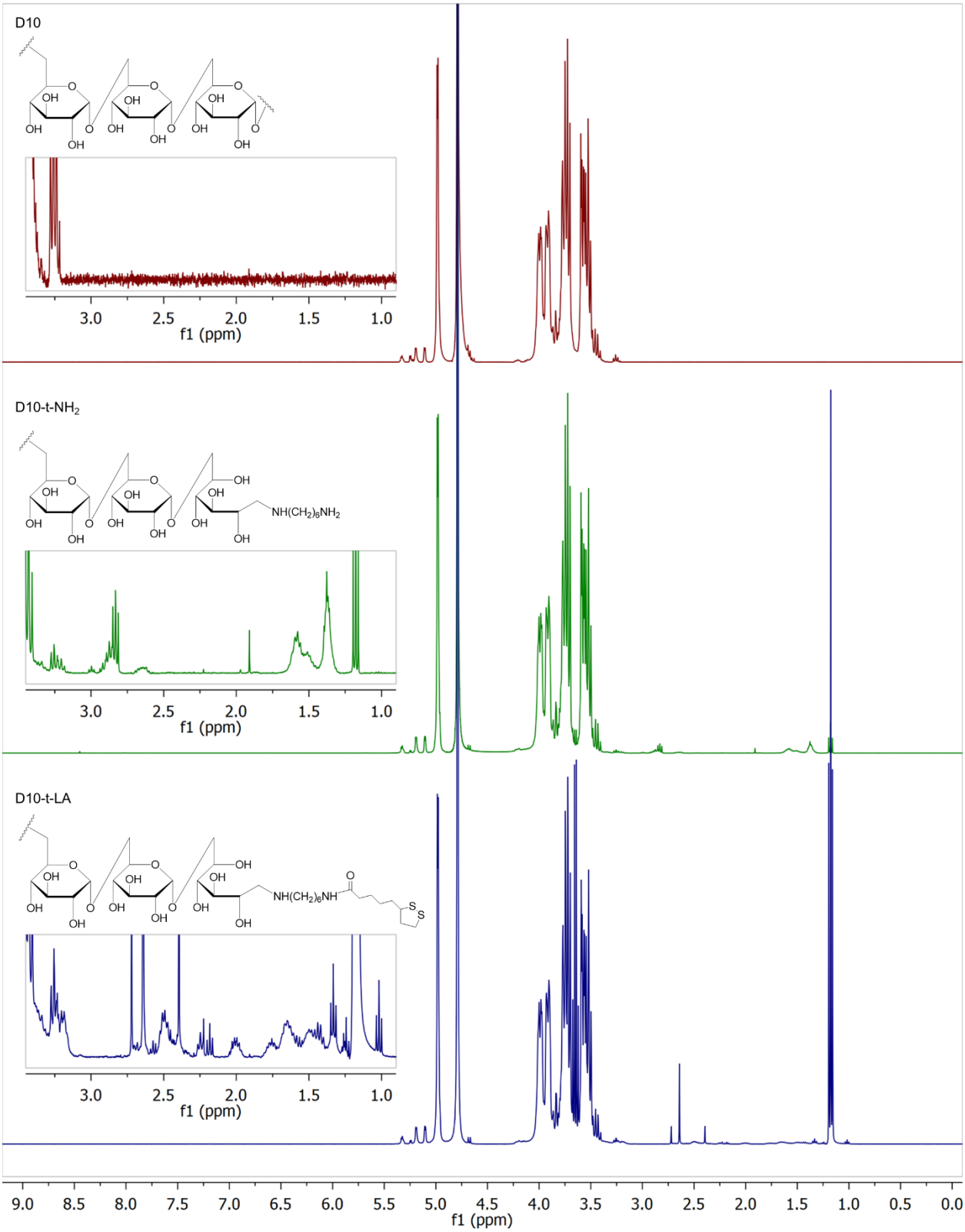

Figure S3. Stacked ^{1}H NMR spectra for D10 (red), D10-t-NH_2 (green), and D10-t-LA (blue). The inset zooms in on 0.9–3.45 ppm.

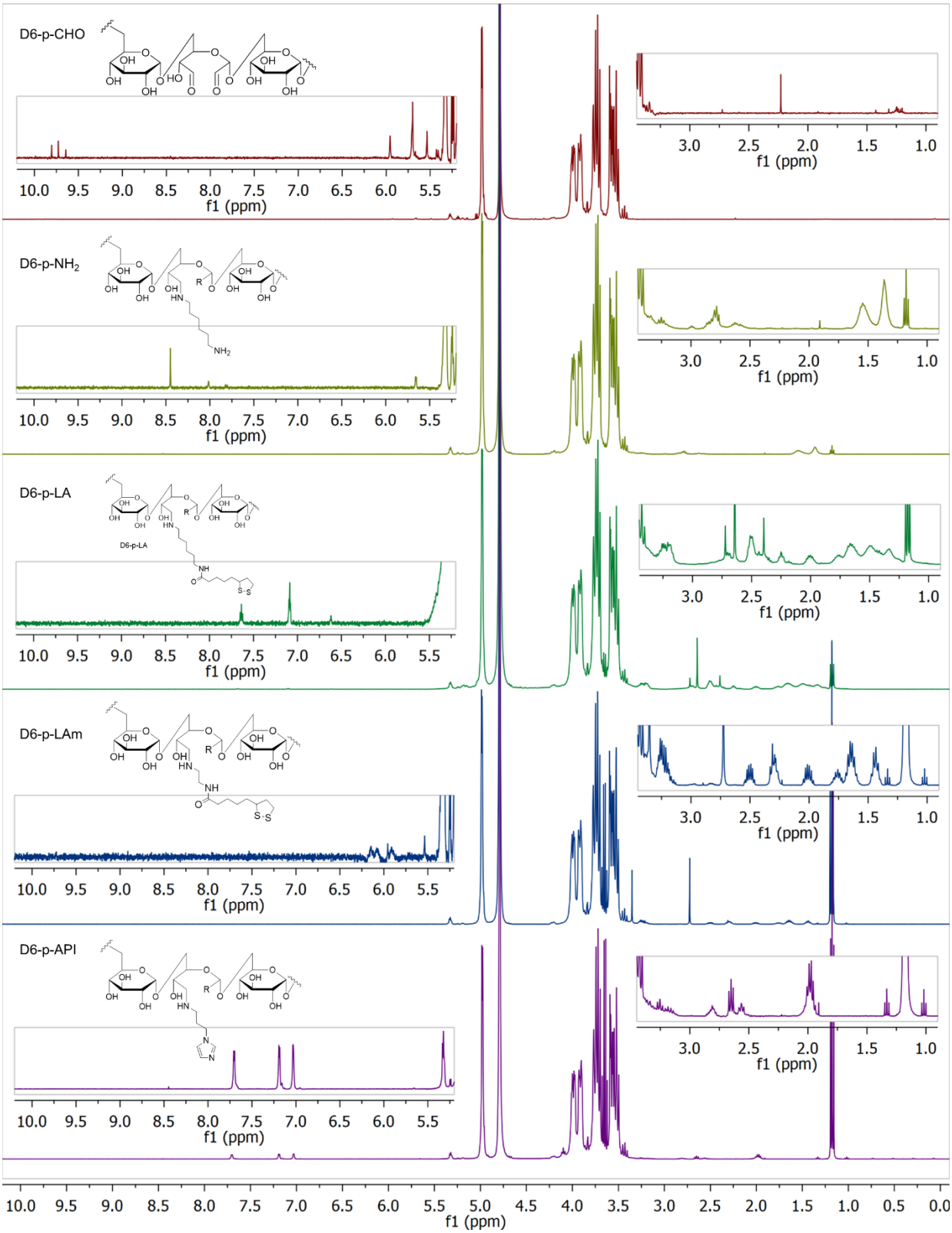

Figure S4. Stacked ^{1}H NMR spectra for D6-p-CHO (red), D6-p-NH_2 (olive), D6-p-LA (green), D6-p-LAm (blue), and D6-p-API (purple). These samples were all prepared from D6 (L). The insets on the left-hand side zoom in on 5.2–10.2 ppm. The insets on the right-hand side zoom in on 0.9–3.45 ppm.

FTIR spectra were measured for the starting materials and modified dextrans (Figure S5). Few differences were observed, with the spectra for all dextrans showing a characteristic C–O stretch at 1010 cm^{-1}. A new peak appeared at ~1570 cm^{-1} for the terminal and pendant samples functionalized with LA and was attributed to the C=O stretch of the newly formed amide bond.

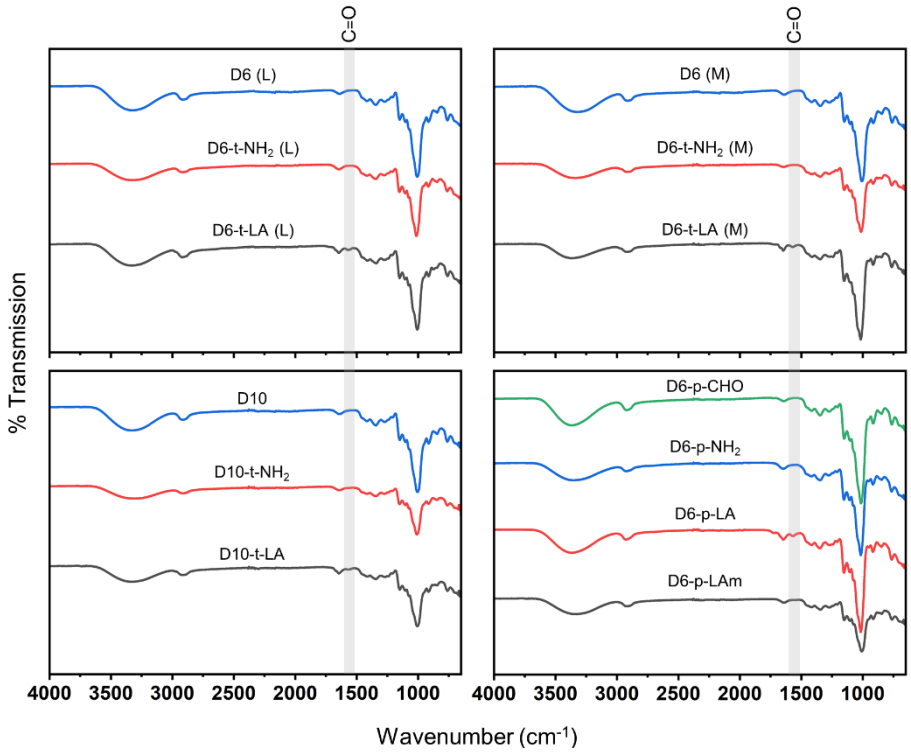

Figure S5. FTIR characterization of dextran and modified dextran ligands. The grey shaded region highlights the region where the LA-associated C=O stretch appears. Top left: D6, D6-t-NH_2, and D6-t-LA from *Leuconostoc* spp. Top right: D6, D6-t-NH_2, and D6-t-LA from *Leuconostoc mesenteroides.* Bottom left: D10, D10-t-NH_2, and D10-t-LA. Bottom right: D6-p-CHO, D6-p-NH_2, D6-p-LA and D6-p-LAm.

The modified dextran ligands, starting materials and intermediates were characterized via colorimetric assays to determine relative amine/thiol content (Table S2). TNBS and Ellman's assays were performed to determine the amine and thiol concentration, respectively. Assuming that both thiols of DHLA would react with the Ellman's reagent, the thiol concentration was divided by two to determine the DHLA concentration. The dextran content of each sample was also determined using an anthrone assay and these values were used to calculate the %NH_2 or

%DHLA per dextran chain. The results showed there was relatively low degrees of functionalization but also showed that both amines and thiols were successfully introduced to the dextran chains.

For the Ellman's assay, the negative controls of HMDA and LA, and the positive control of GSH, were prepared at concentrations of ~100 μM. These controls gave thiol (SH) concentrations of < 0 μM, 2.5 ± 3.7 μM, and 93 ± 2 μM, respectively, confirming selectivity for thiols (and not amines or disulfides).

Table S2. Quantification of relative amine (NH_2) and thiol (DHLA) per dextran ligand determined by the TNBS and Ellman's assay, respectively. The actual thiol concentration was divided by two, assuming that each DHLA ligand has two thiol groups.

Ligand	%NH_2/Dex (TNBS)	%DHLA/Dex (Ellman's)
D6 (L)	0.2 ± 0.06	–0.2 ± 0.1
D6-t-NH_2 (L)	1.4 ± 0.1	--
D6-t-LA (L)*	–0.1 ± 0.01	6.9 ± 0.2
D6 (M)	0.3 ± 0.02	–0.1 ± 0.02
D6-t-NH_2 (M)	3.3 ± 0.1	--
D6-t-LA (M)*	2.1 ± 0.04	7.4 ± 0.3
D10	0.0 ± 0.3	–0.1 ± 0.5
D10-t-NH_2	56 ± 4	--
D10-t-LA*	0.7 ± 0.04	11 ± 1
D6 (L)	0.2 ± 0.06	–0.2 ± 0.08
D6-p-CHO	–1.3 ± 0.06	--
D6-p-NH_2	37 ± 2	--
D6-p-LA*	1 ± 0.03	29 ± 1
D6 (L)	0.2 ± 0.06	–0.2 ± 0.08
D6-p-CHO	–1.3 ± 0.06	--
D6-p-LAm*	1.9 ± 0.06	23 ± 2

The * indicates that these ligands were reduced to DHLA (as described above) for the Ellman's assay. The Ellman's assay results for oxidized dextran were negative (no significant color change) but are not listed in this table because an anthrone assay was not done in parallel to quantitate the amount of dextran.

Ninhydrin colorimetric tests were also performed to test for amines (Figure S6). Upon mixing and heating the ligand with ninhydrin, a purple color (Ruhemann's purple) is observed if primary amines are present, and the intensity of the purple color is proportional to the relative amine concentration.[26] As expected, the amine-modified dextrans turned purple upon reaction with ninhydrin. The LA-modified ligands did not turn purple (except D6-p-LA which was very faintly purple) when mixed with ninhydrin, indicating successful reaction of the amine groups with LA-NHS.

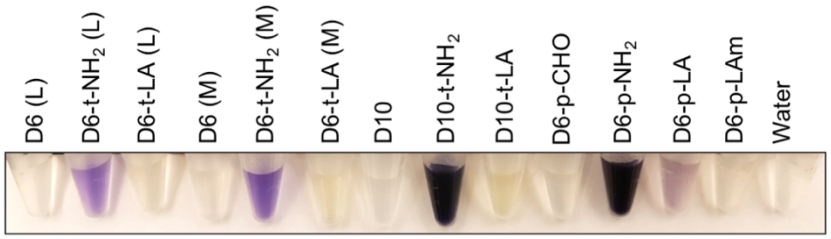

Figure S6. Ninhydrin colorimetric test for primary amines with various modified dextran ligands. The purple color is formed upon reaction of ninhydrin with primary amine groups. The intensity of the purple color is proportional to the relative concentration of amine groups.

Ligand Exchange. Figure S7 (next page) shows a cartoon schematic for the two-step ligand exchange procedure for preparing Dex-QDs from hydrophobic, organic-phase QDs that were primarily coated with trioctylphosphine oxide (TOPO).

Characterization of Dex-QDs

Infrared Absorption

FTIR spectra were measured for X-QD samples where X = histidine, D10-t-DHLA, D6-t-DHLA, D6-p-DHLA, D6-p-DHLAm, and D6-p-API (Figure S8, next page). These spectra showed that the ligand exchanges were successful as peaks corresponding to histidine or dextran could be observed. The peaks for histidine were notably broadened with the QD samples, indicating that the histidine was bound. The dextran peaks did not have noticeable broadening when bound to the QDs, likely because the peaks were already broadened by the polymeric nature of the material.

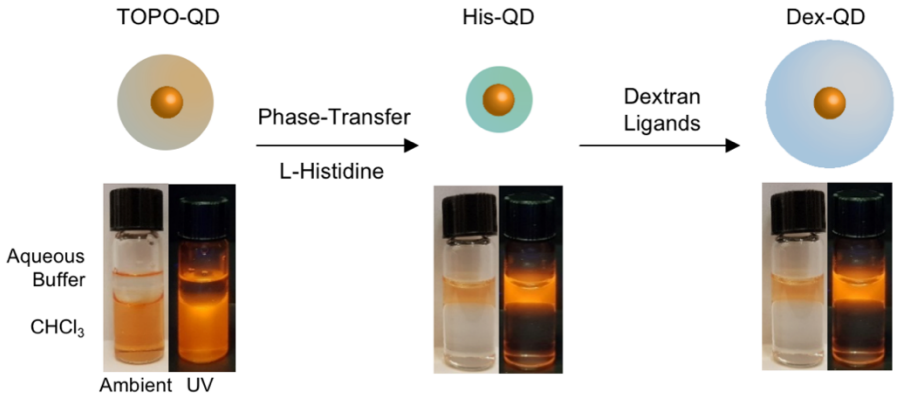

Figure S7. Cartoon showing the two-step ligand exchange procedure to prepare dextran-functionalized QDs (Dex-QDs). The photos show the organic-aqueous phase preference of the QDs. Histidine (His) is used as a weakly coordinating ligand to facilitate transfer of the organic QDs to the aqueous phase. The His ligands are then displaced with more strongly coordinating dextran ligands.

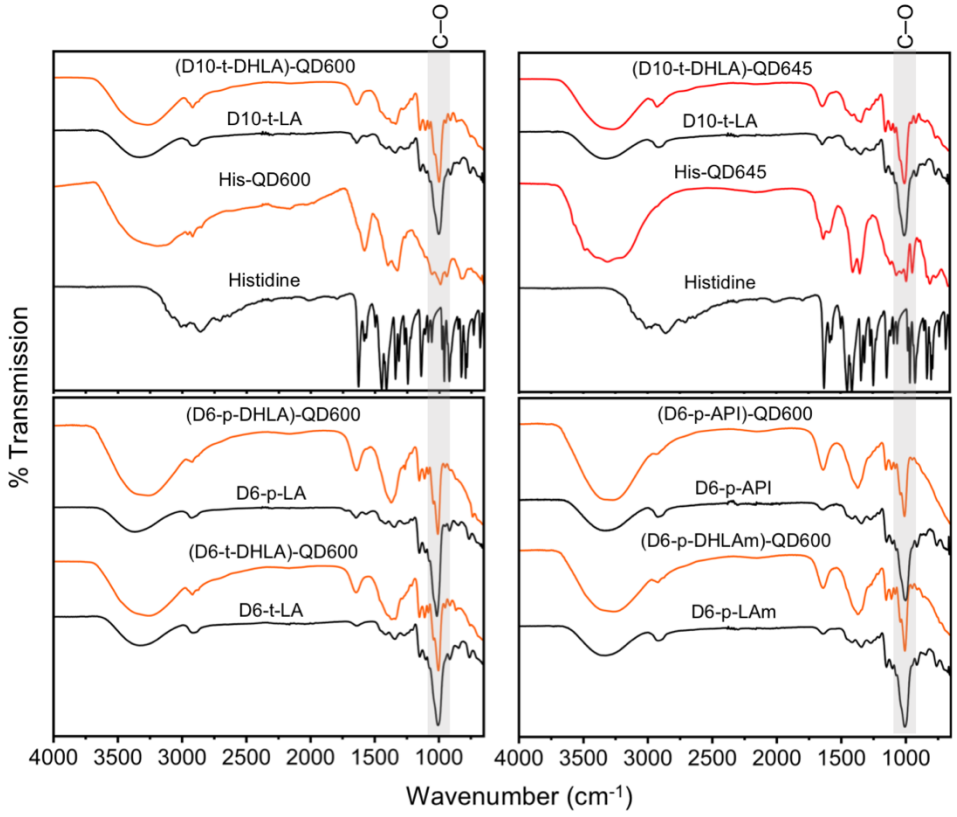

Figure S8. FTIR characterization of modified dextran ligands and Dex-QDs. Top panels: Comparison between the ligands histidine and D10-t-LA and QDs coated with these ligands for QD600 (left) and QD645 (right). Bottom left: D6-t-LA and D6-p-LA ligands and QD600 coated with these ligands. Bottom right: D6-p-API and D6-p-LAm ligands and QD600 coated with these ligands. The grey shaded region highlights the C–O stretch of dextran.

Functional Tests

Anthrone assays were done to determine the amount of dextran present on X-QD600, where X = DHLA or a modified dextran. DHLA-QDs were used as a control to confirm that anthrone was insensitive to the QDs themselves. All of the Dex-QDs showed positive results upon reaction with anthrone, indicating successful functionalization with the ligands. Using the size of the QDs determined by TEM, an assumption of spherical morphology, and the estimated QD concentration, the number of dextran ligands per QD was estimated (Figure S9). The D-t-DHLA ligands showed higher grafting densities than the pendantly modified ligands, which could be due to the different conformations of the dextran. Overall, the grafting density is high compared to what has previously been reported for other ligands.[27,28] For this reason, a control experiment was done where DHLA-QD600 were mixed with unmodified dextran (D6 (L)) and then purified via spin filtration analogous to the workup for preparing Dex-QDs. An anthrone assay was then done on these QDs and confirmed that >97% of the dextran added was removed during the purification process. We are thus uncertain as to the reason for the high densities of dextran per QD, but speculate that some dextran entanglement may have occurred around the QDs such that there was a large number of chains associated per QD but not all was coordinated to the nanocrystal surface. Entanglement of dextran chains has been reported previously.[29–31]

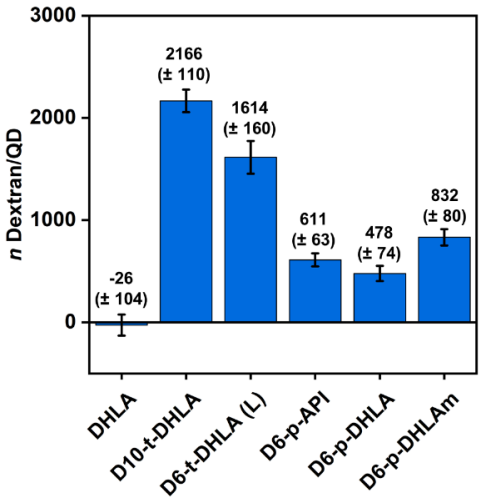

Figure S9. Anthrone assay for determining the number of dextran ligands per QD. The values are calculated based on quadruplicate measurements, and are expressed as the mean (± 1 standard deviation).

The ConA-induced aggregation of Dex-QDs was also used to verify successful functionalization. These results are mainly presented in Figure 2 (main text). Figure S10 shows magnified views of the photographs from Figure 2. Figure S11 shows that BSA (pI 4.7) and lysozyme (Lyz; pI 10.7) did not induce aggregation. These proteins had net negative and net positive charges, respectively, under the conditions of the experiment. For this experiment, a 50 nM solution of (D10-t-DHLA)-QD600 was prepared with 100 molar equivalents of ConA, BSA, or Lyz in PBS buffer supplemented with Ca^{2+} and Mn^{2+} ions. The samples were incubated for 30 min, and then loaded in an agarose gel, which was run at a field strength of ~6.7 V cm^{-1} for 30 min.

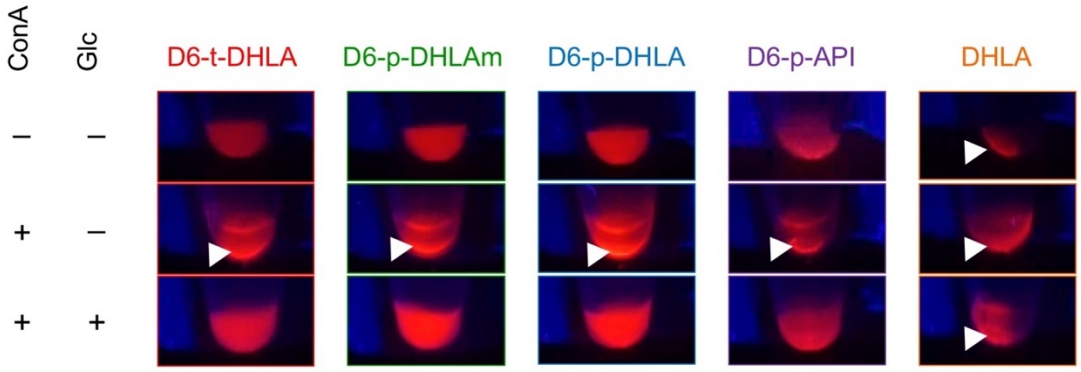

Figure S10. Magnified view of the photographs from Figure 2. X-QD solutions without (–) ConA, with (+) ConA, and with both ConA and glucose (Glc). The white arrows indicate aggregates. DHLA-QDs were used as a non-dextran control and Glc was used for competitive binding with ConA. Any appearance of settled aggregates for the D6-p-API (ConA –, Glc –) and (ConA +, Glc +) samples is largely an artefact of the photography.

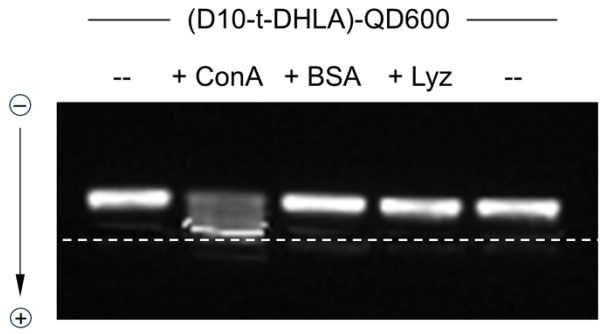

Figure S11. (D10-t-DHLA)-QD600 incubated with 100 molar equivalents of dextran-specific (ConA) and non-specific (BSA, Lyz) proteins. Wells are labeled with a white dashed line. Agarose gels were prepared as a 0.5% (w/v) solution in TBE buffer. Gels were run at ~6.7 V cm^{-1} for 30 min.

Specific binding and elution of Dex-QDs with ConA-sepharose were also tested (Figure S12). ConA-sepharose is an affinity resin that binds molecules containing α-D-mannopyranosyl, α-D-glucopyranosyl, and other sterically similar sugar molecules. Elution of specifically bound analytes was achieved using a solution of D-glucose. Dex-QDs (D6-t-DHLA and D3.5-t-DHLA) were tested along with control samples of His- and DHLA-QDs. His-QDs bound non-specifically to the resin, but could be washed off with a solution containing 1.5% BSA. When (D3.5t-DHLA)-QD630 were mixed with the resin and exposed to the same BSA wash, no elution was observed, indicating specific binding between the dextran coating on the QDs and the ConA sepharose. Elution of the (D3.5-t-DHLA)-QD630 was achieved using a 0.5 M D-glucose solution. Control samples of DHLA-QDs bound non-specifically and irreversibly to the resin, whereas (D6-t-DHLA)-QD645 were bound and successfully eluted with 0.5 M D-glucose under the same binding and elution conditions.

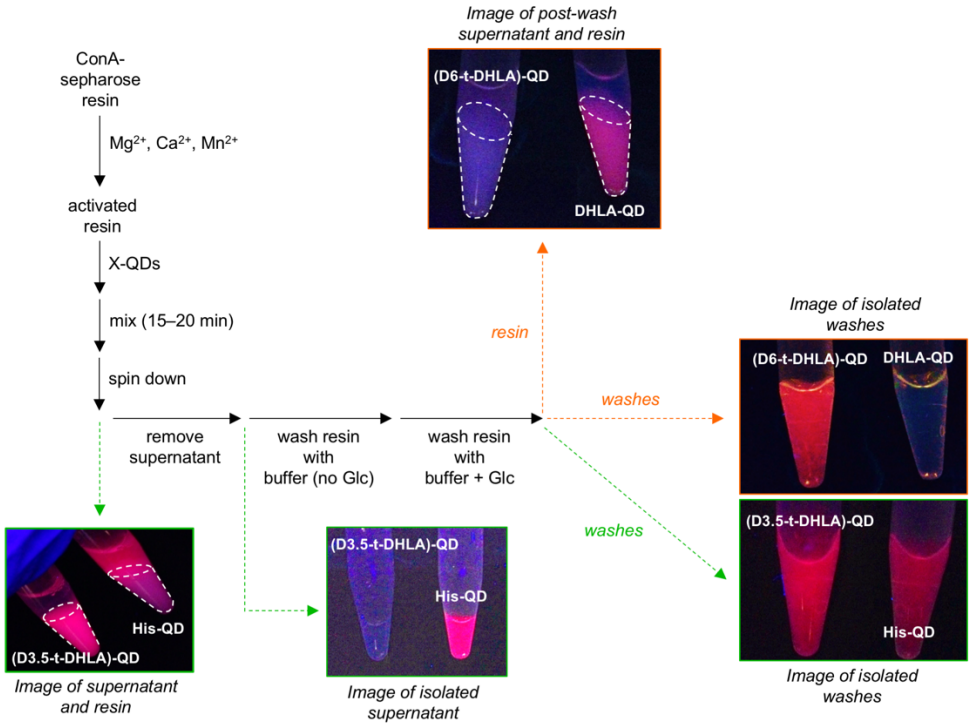

Figure S12. Flow chart illustrating tests of the specific binding and elution of Dex-QDs to and from ConA-sepharose resin. Photographs taken under UV illumination show the PL intensities of the resin and/or supernatant/washes at important points in the tests. The dashed lines outline the resin in the tubes. Experiments were done with His-QD (green dashed arrows) and DHLA-QD (orange dashed arrows) as controls. (Black solid arrow represent common steps in both experiments.)

Optical Characterization

Figure S13 shows the plots of normalized absorbance, PL emission and PL excitation spectra of the CdSe/ZnS and CdSe/CdS/ZnS QDs used.

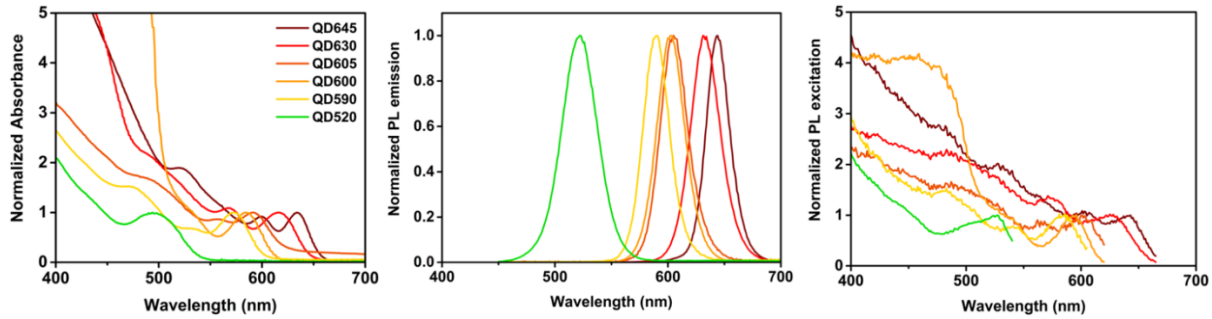

Figure S13. Normalized absorbance, emission, and excitation spectra for the QDs utilized in this study. The absorbance and excitation spectra are normalized to the first-exciton peak.

Quantum Yield (QY)

Figure S14 shows the plots of integrated PL intensity versus absorbance used for the estimation of PL QY values for QD600 samples with different ligand coatings using fluorescein as a reference. The determined QY values are provided in Table S3.

Table S3. PL QY for QD600 samples.

Ligand	QY (%)
Fluorescein	93
Histidine	28
D6-t-DHLA	13
D10-t-DHLA	9
D6-p-DHLAm	18
D6-p-DHLA	20
D6-p-API	29
DHLA	10
GSH	28

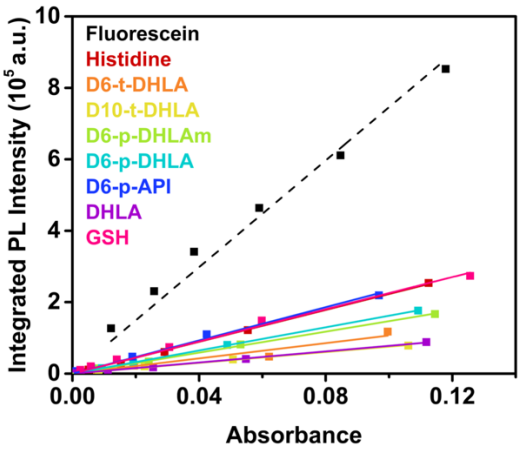

Figure S14. Quantum yield measurements with various X-QDs. The data is the integrated PL emission intensity for samples of each material plotted against the corresponding absorbance. Fluorescein in borate buffer was used as a reference standard.

Size Characterization

Figure S15 shows example TEM images of QD600 and QD645. The size of 50 individual QDs (including core/shell/shell structure) was measured and averaged.

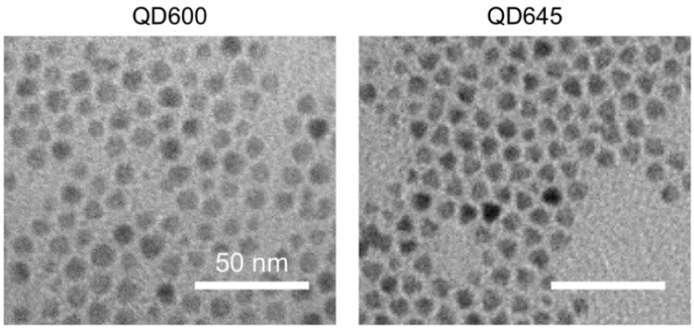

Figure S15. Representative TEM images of QD600 and QD645. These QDs were used most frequently throughout this study. The scale bar is 50 nm.

Figure S16A shows representative number-weighted size distributions collected via DLS for X-QD600 samples (X = D6-t-DHLA (L) and (M), D6/10-t-DHLA, D10-t-DHLA, D6-p-DHLA, D6-p-DHLAm, D6-p-API, DHLA, GSH, and His) in bicarbonate buffer. (All D6-p- ligands were prepared from D6 (L).) The size distributions were averaged over at least three replicate measurements.

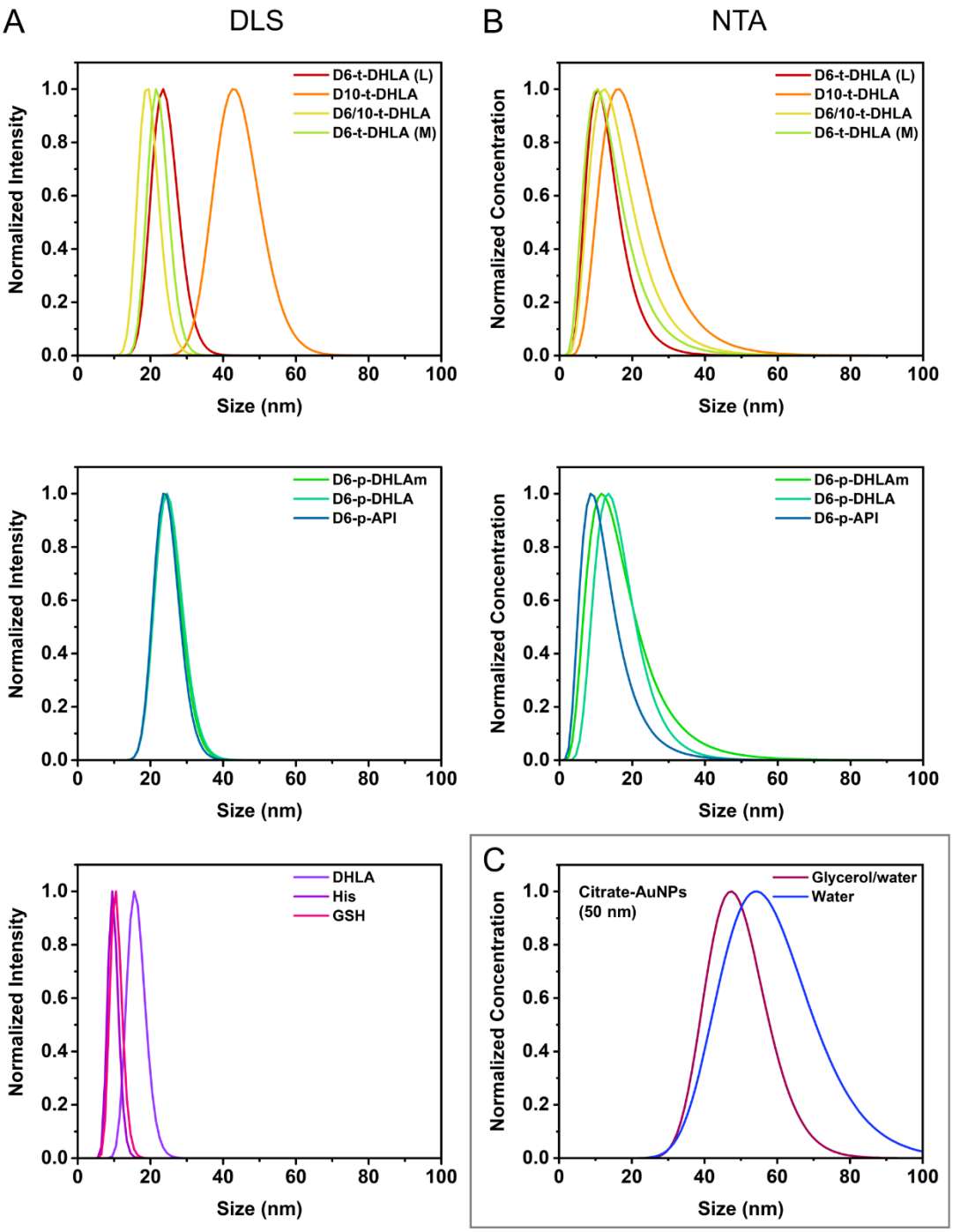

Figure S16. (A) DLS measurements on various Dex-QD600 and QD600 coated with small molecule ligands. The samples were dispersed in aqueous buffer. **(B)** NTA measurements of Dex-QDs dispersed in glycerol/water solution (40% v/v glycerol). **(C)** NTA measurements of nominal 50 nm-diameter, citrate-coated AuNPs in glycerol/water solution (40% v/v glycerol) and water.

Figure S16B shows representative size distributions collected via NTA for Dex-QD600 samples in glycerol/water solution (40% v/v glycerol).

NTA analysis was also performed on 50 nm-diameter, citrate-coated AuNPs via scattering mode in both water and glycerol/water mixtures (40% v/v glycerol). The measurements were performed in triplicate, fitted with a lognormal distribution, and the mean size values were averaged. As shown in Figure S16C, the solvodynamic size in water was larger (59 ± 3 nm) than in 40% v/v glycerol (*aq*) (49 ± 1 nm). Using these values, a correction factor was determined with the mean value in water being ~20% larger than that in 40% v/v glycerol (*aq*). This correction factor was applied to the NTA data for the QDs and the corrected values are provided in Table 1 (main text).

Electrophoretic Mobility

Figure S17 (next page) shows example agarose gels of different QD samples with different ligand coatings and colors of QDs. Similar trends were observed between different batches of QDs.

Assessing Non-Specific Binding

Non-specific binding to proteins

Figure S18 shows agarose gels of GSH-QD645 and His-QD600 incubated with 1.0, 5.0 or 9.5 mg/mL protein solutions of BSA, lysozyme, or casein (as skim milk powder) and 10%, 50% or 95% v/v plasma solution. Both of these QD samples show large amounts of non-specific binding to the proteins, as indicated by the large mobility shifts (BSA, casein, plasma) and aggregation (lysozyme). These results are in contrast to the gel images for Dex-QDs shown in Figure 5 (main text), which show much lower amounts of non-specific binding, with the exception of (D6-p-API)-QDs. Table S4 elaborates on how general observations regarding the agarose gels in Figure S18 and Figure 5 are physically interpreted. Table S5 details the specific observations and interpretations for each combination of protein and X-QD.

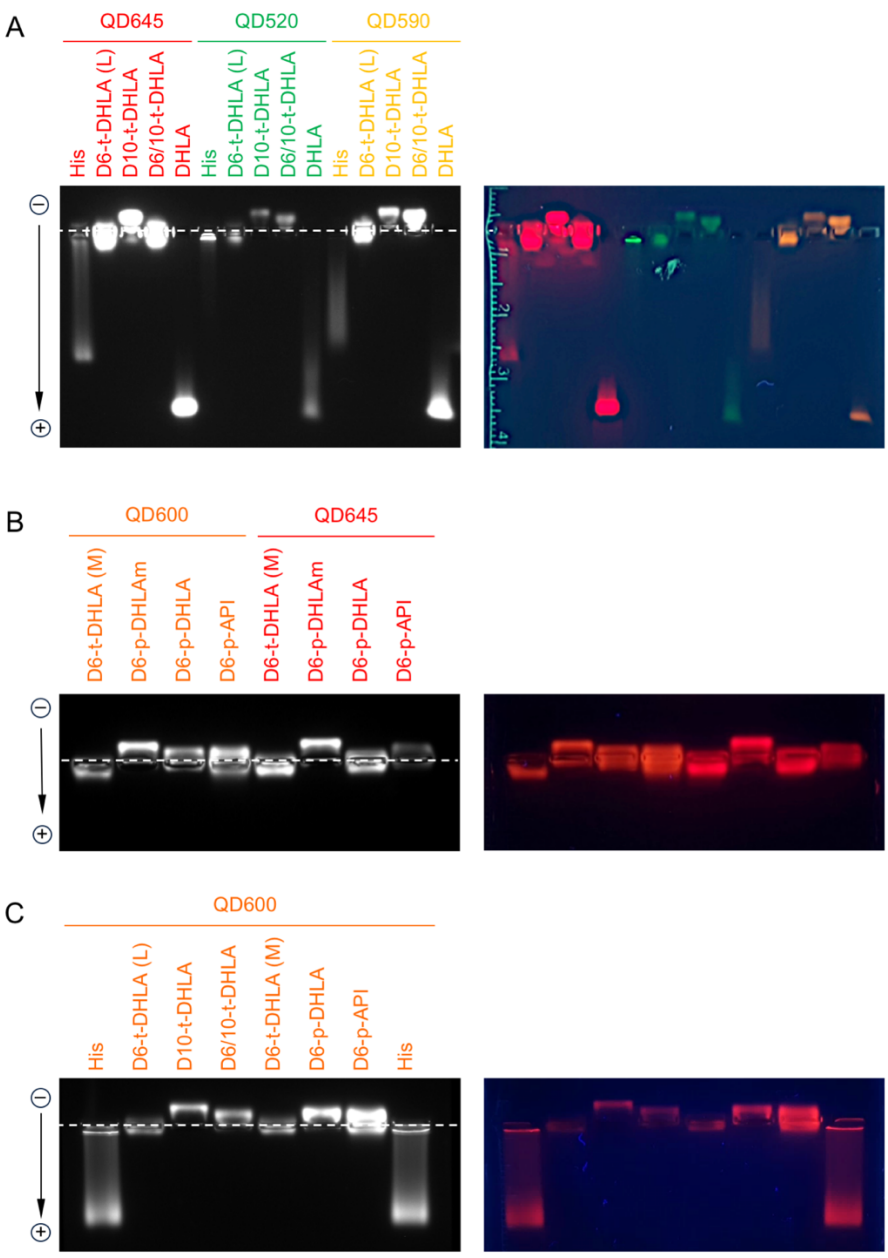

Figure S17. Agarose gel electrophoresis results for multiple colors of QDs coated with histidine, DHLA, or the dextran ligands. The images in the left column are monochrome images acquired under UV-illumination (via a gel imager). The images on the right are RGB color images acquired under UV-illumination (via a smartphone).

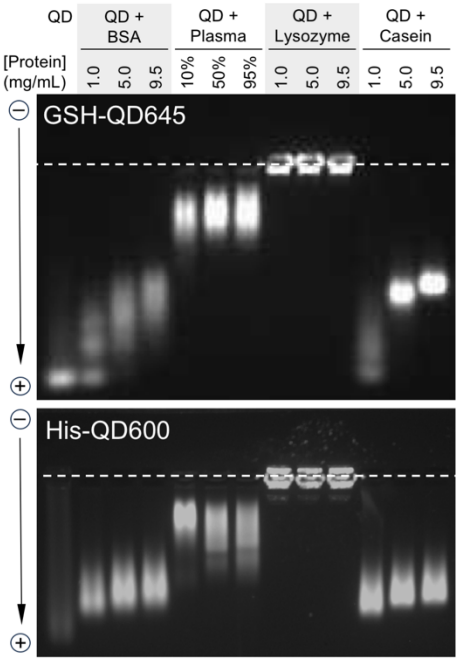

Figure S18. Agarose gels of X-QDs after incubation with 1.0, 5.0 and 9.5 mg/mL protein solutions (in bicarbonate buffer, excluding plasma, which is percent v/v), where X = GSH or His. The QDs showed strong non-specific binding.

Table S4. General interpretation of agarose gel electrophoresis data with respect to protein adsorption.

Observation	Applicable Ligands	Interpretation(s)
Decrease in anodic mobility	DHLA, GSH, His	Increase in size from adsorbed protein *and/or* Reduction of net charge from adsorption of positively charged protein
Increase in anodic mobility	Dex	Increase in net charge from adsorption of negatively charged protein
Increase in cathodic mobility	Dex	Increase in net charge from adsorption of positively charged protein
Increased band streaking	DHLA, GSH, Dex	Dynamic interactions (*i.e.* weak binding and unbinding) *and/or* Unresolved populations with different numbers of adsorbed proteins
Decreased band streaking	His	Replacement of a less stable nanoparticle coating with a more stable one
Multiple bands	All	Populations with different numbers of adsorbed proteins.
Small changes in observations with increasing protein concentration	All	Weak and minimal adsorption of protein (if similar overall mobility to negative control sample) *or* Strong and saturated adsorption of protein (if much different overall mobility than negative control sample)
Large changes in observations with increasing protein concentration	All	Moderate adsorption (if protein equivalents in large excess of nanoparticle equivalents) *or* Strong adsorption (if protein equivalents not in large excess)

Table S5. Detailed interpretations of agarose gels in Figure 5 and Figure S18. The reference points for the observations are the samples of QDs that are not mixed with proteins.

Ligand	Protein(s)	Observations	Qualitative Conclusion
DHLA (Fig. 5)	BSA	• 33–50% decrease in anodic mobility • Approaches saturated effect between 5 and 9.5 mg/mL protein • Moderate streaking	Moderate-to-strong adsorption
	Plasma	• ~80% decrease in anodic mobility • Saturated effect across all plasma concentrations • Moderate streaking	Strong adsorption
	Lysozyme	• Complete loss of mobility at all protein concentrations	Strong adsorption
	Casein	• 40–50% decrease in anodic mobility • Saturated effect at 5 and 9.5 mg/mL protein • Very little streaking	Strong adsorption
D10-t-DHLA (Fig. 5)	BSA	• Consistent fraction of QDs with unchanged mobility • A fraction of QDs shows a slight increase in anodic mobility that does not change much between protein concentrations	Weak adsorption
	Plasma	• Moderate streaking • Small cathodic mobility becomes anodic mobility when proteins added • Small increase in anodic mobility as protein concentration increases	Moderate-to-strong adsorption
	Lysozyme	• Small increase in cathodic mobility • The increase in cathodic mobility scales with protein concentration	Moderate adsorption
	Casein	• No changes in mobility	Weak (if any) adsorption
D6-p-DHLA (Fig. 5)	BSA	• Very slight anodic increase in band streaking	Weak adsorption
	Plasma	• Clear increase in anodic mobility and band streaking as protein concentration increases	Strong adsorption
	Lysozyme	• Consistent fraction of QDs with unchanged mobility • Very small fraction of QDs with increasing cathodic mobility as protein concentration increases	Weak adsorption
	Casein	• Substantial increase in anodic mobility and band streaking • Saturated effect at 5 and 9.5 mg/mL protein	Strong adsorption

D6-p-API (Fig. 5)	BSA	• Small fraction of QDs with unchanged mobility at 1 mg/mL protein • Small cathodic mobility becomes anodic mobility when protein added • Progressive increase in cathodic mobility and band streaking as protein concentration increases	Moderate adsorption
	Plasma	• Small cathodic mobility becomes anodic mobility when protein added • Small increase in anodic mobility and streaking as protein concentration increases • Appearance of a non-mobile fraction of QDs when mixed with protein	Strong adsorption
	Lysozyme	• No change in mobility at 1 and 5 mg/mL protein	Weak adsorption
	Casein	• Small cathodic mobility becomes a very large anodic mobility when protein added • Large increase in band streaking • Appearance of an immobile fraction of QDs at 5 and 9.5 mg/mL protein • Saturated effects at 5 and 9.5 mg/mL protein	Strong adsorption
GSH (Fig. S18)	BSA	• Progressive decrease in anodic mobility with increasing protein concentration • Resolution of multiple bands at 1.0 mg/mL protein • Fraction with unchanged mobility at 1.0 mg/mL protein	Moderate adsorption
	Plasma	• ~80% decrease in anodic mobility • Moderate band streaking • Saturated effect at 50% and 95% plasma	Strong adsorption
	Lysozyme	• Complete loss of mobility at all concentrations	Strong adsorption
	Casein	• At 1.0 mg/mL, a fraction of QDs with unchanged mobility and streaking for a band with decreased anodic mobility • ~45% decrease in anodic mobility at 9.5 mg/mL protein	Strong adsorption
His (Fig. S18)	BSA	• Decrease in band streaking • Up to 25% decrease in anodic mobility • Approaching a saturated effect between 5 and 9.5 mg/mL of protein	Strong adsorption
	Plasma	• Large decrease in streaking and ~75% decrease in anodic mobility at 1 mg/mL • Increase in anodic mobility and streaking (relative to 1 mg/mL) at 5 and 9.5 mg/mL of protein	Strong adsorption
	Lysozyme	• Complete loss of mobility at all concentrations.	Strong adsorption
	Casein	• Decrease in band streaking • Up to ~25% decrease in anodic mobility • Approaching a saturated effect between 5 and 9.5 mg/mL protein	Strong adsorption

Non-specific binding to cells

Figure S19 shows PL and brightfield microscopy images of A549 and MDA-MB-231 cells that were incubated with 50 nM X-QD600 samples. Cells that were not incubated with QDs were used as a negative control. All of the Dex-QDs showed minimal non-specific binding compared to the GSH-QDs. Figure S20 shows the control samples for the quantitative non-specific binding assay. Empty sample wells were incubated with different amounts of QDs. The QDs had minimal binding to the sample wells themselves.

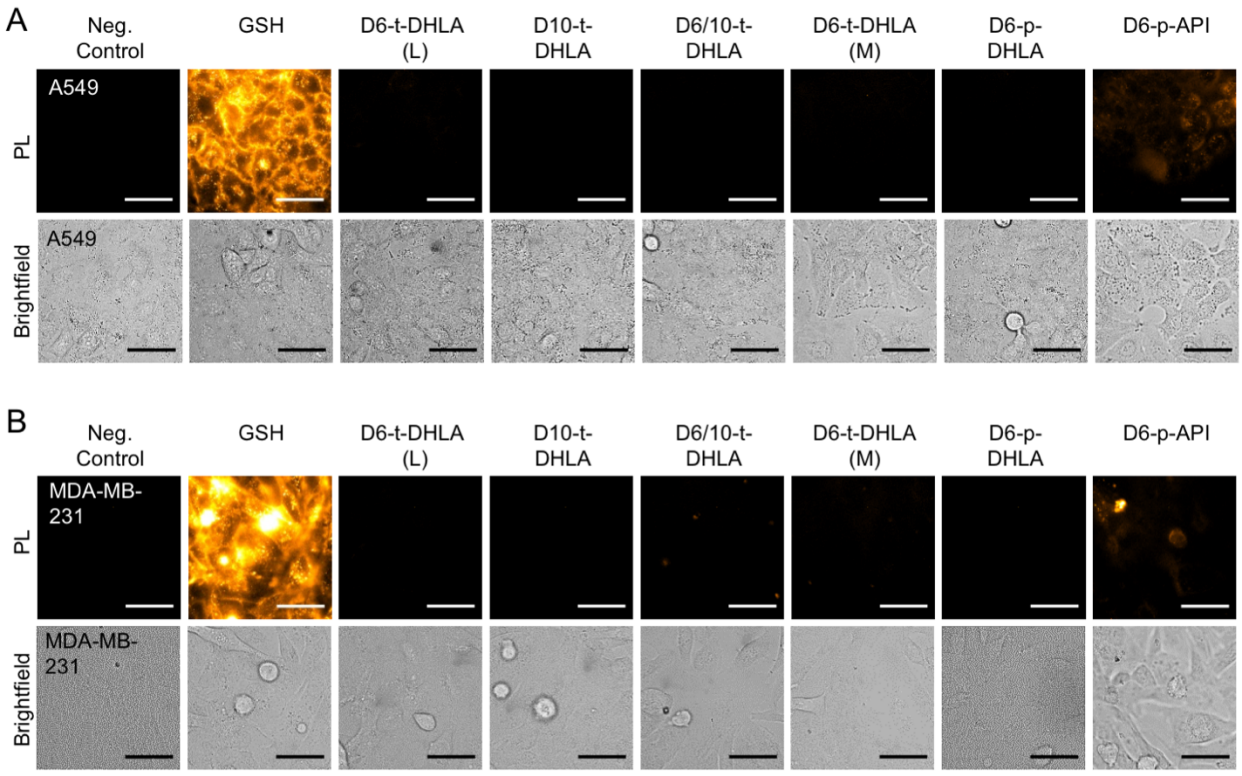

Figure S19. Comparison of non-specific binding between live cells and QD600 (50 nM) with various ligand coatings. Images were acquired under brightfield and fluorescence modes. **(A)** A549 cells. **(B)** MDA-MB-231 cells. Negative controls are cells that were not incubated with QDs. Scale bar = 50 μm. Exposure time = 150 ms. Images were acquired at the same microscope and camera settings.

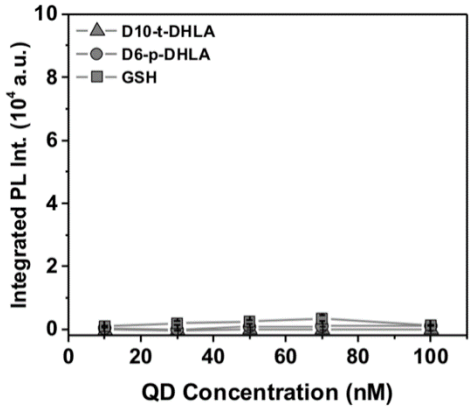

Figure S20. Quantitative assay of empty wells in a well plate incubated with increasing concentrations of QDs (after washing).

Cellular Microinjection. Figure S21 shows PL and brightfield microscopy images of attempted microinjections of DHLA-QD600 into A549 cells. The QDs remained at the injection site, did not disperse in the cytosol of the cell, and the PL from the injection site quickly faded.

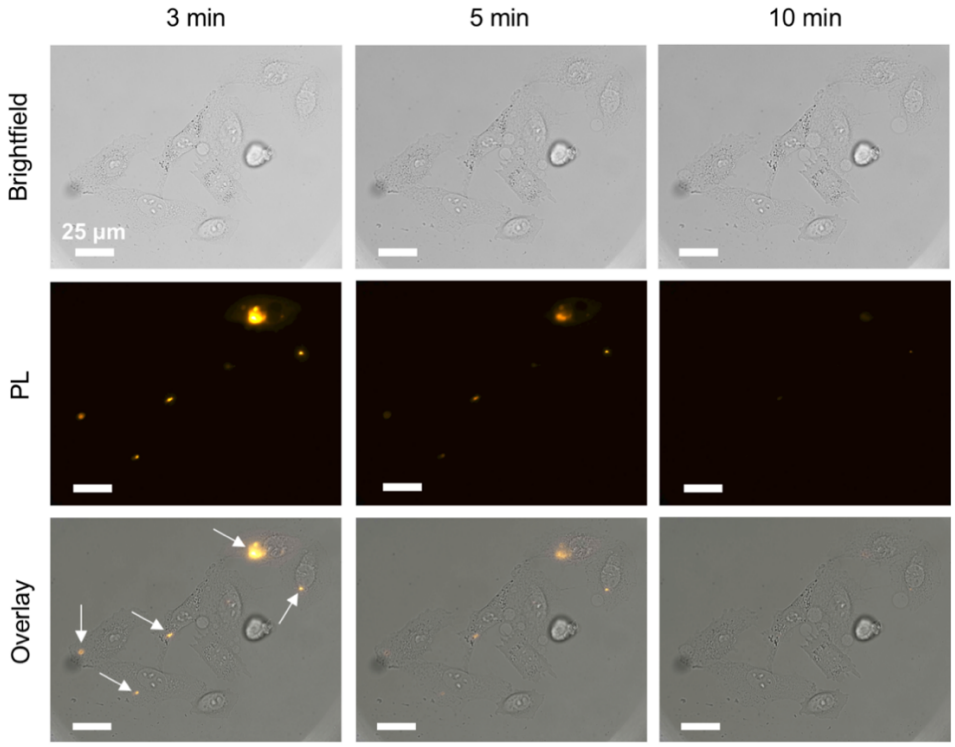

Figure S21. Brightfield, PL, and overlay images of DHLA-QD600 samples after attempted microinjections (arrows) into A549 cells. The scale bars are 25 µm.

Covalent Conjugation and pH Sensing. Figure S22 shows PL emission spectra for the corresponding gel bands of FITC-labeled Dex-QDs. The gel image is reproduced from Figure 9 (main text). The PL emission spectra for FITC and QD600 samples (individually) at different pH values are shown in Figure S23.

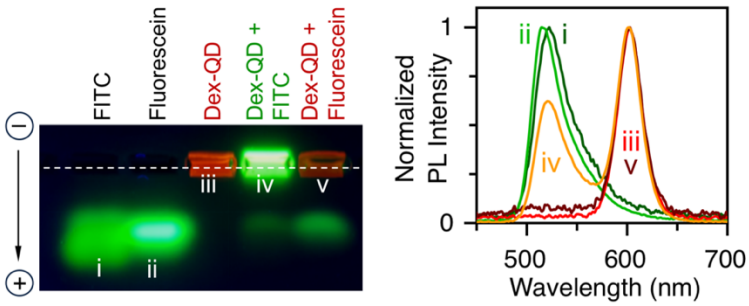

Figure S22. PL image of an agarose gel of FITC-labeled Dex-QDs and the PL emission spectra measured for each of the gel bands (labeled with Roman numerals).

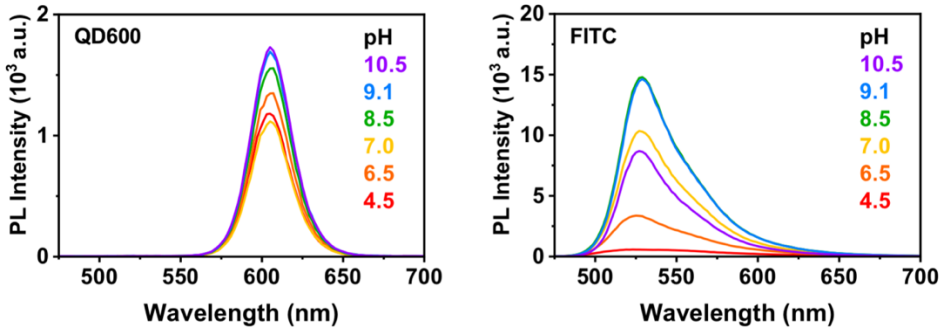

Figure S23. Emission spectra for (D6-t-DHLA)-QD600 (left) and FITC (right) at various pH values.

Peptide Assembly

Self-assembly on QDs

Dex-QD600 samples (D10-t-DHLA, D6-p-DHLA, D6-p-DHLAm, and D6-p-API) were incubated with 0, 5, 10, 20 or 30 equivalents of A647-labeled, hexahistidine-tagged peptides (entry 2 in Table S1). The peptide contained four aspartic acid residues and imparted a net negative charge to the QDs upon binding. The A647 dye was also a FRET acceptor for the QD600. Figure S24 shows PL emission spectra and images of agarose gels for various Dex-QDs

mixed with the peptides. Assembly between the peptides and QDs was indicated by the observation of progressive quenching of QD PL emission with an increasing number of peptides per QD, and parallel increases in A647 PL emission, consistent with FRET. (Direct excitation of the A647 was negligible.) Assembly was further indicated by progressive increases in the electrophoretic mobility of the QDs with an increasing number of peptides. This mobility was consistent with negative charge added by the assembled peptides.

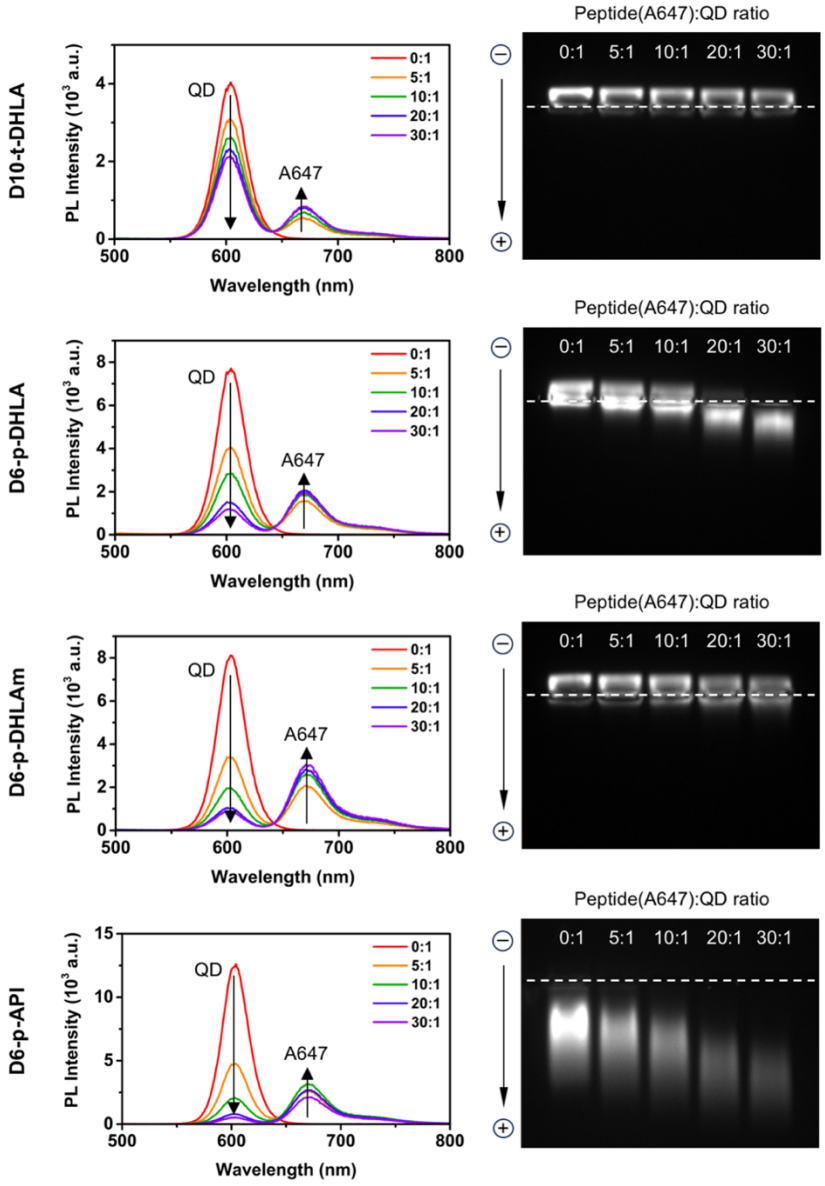

Figure S24. PL emission spectra (left) and PL images of agarose gels (right) for Dex-QDs mixed with varying equivalents of A647-labeled peptide. The peptide sequence includes an anionic tetraaspartic acid tract.

Enzyme Kinetics

Figure S25 (next page) shows normalized FRET-based progress curves for the protease-catalyzed hydrolysis of peptide-(X-QD605) conjugates. The proteases were trypsin and plasmin. Some of this data is shown in Figure 10 (main text). GSH-QDs were used as a reference material for comparison to Dex-QDs. All of the Dex-QDs showed slower hydrolysis than the GSH-QDs. Many factors affect the rate of protease-catalyzed hydrolysis, including steric hindrance,[32] so this result was expected as the dextran ligands are much larger than GSH.

Table S6 tabulates the estimated k_{cat}/K_M values extrapolated, via Eqn. S4, from the data in Figure S25. The terms in Eqn. S4 are the initial rate, v_0, the Michaelis constant, K_M, the turnover number, k_{cat}, and the enzyme and substrate concentrations, $[E]$ and $[S]$. We took $[S]$ to be equal to the concentration of QDs (50 nM).

$$v_0 \approx \frac{k_{cat}}{K_M}[E][S] \qquad \text{(S4)}$$

Table S6. Estimated specificity constants, k_{cat}/K_M ($mM^{-1}\ s^{-1}$).

	D10-t-DHLA	D6-t-DHLA	D6-p-DHLA	D6-p-API	GSH
Trypsin					
nsLys	0.06	0.2	0.7	0.2	5
nsArg	0.3	0.5	1	0.4	17
Plasmin					
nsLys	nd	0.2	2	0.1	30
nsArg	nd	nd	0.2	nd	2

nd = not determined (rate too slow or not measurable)

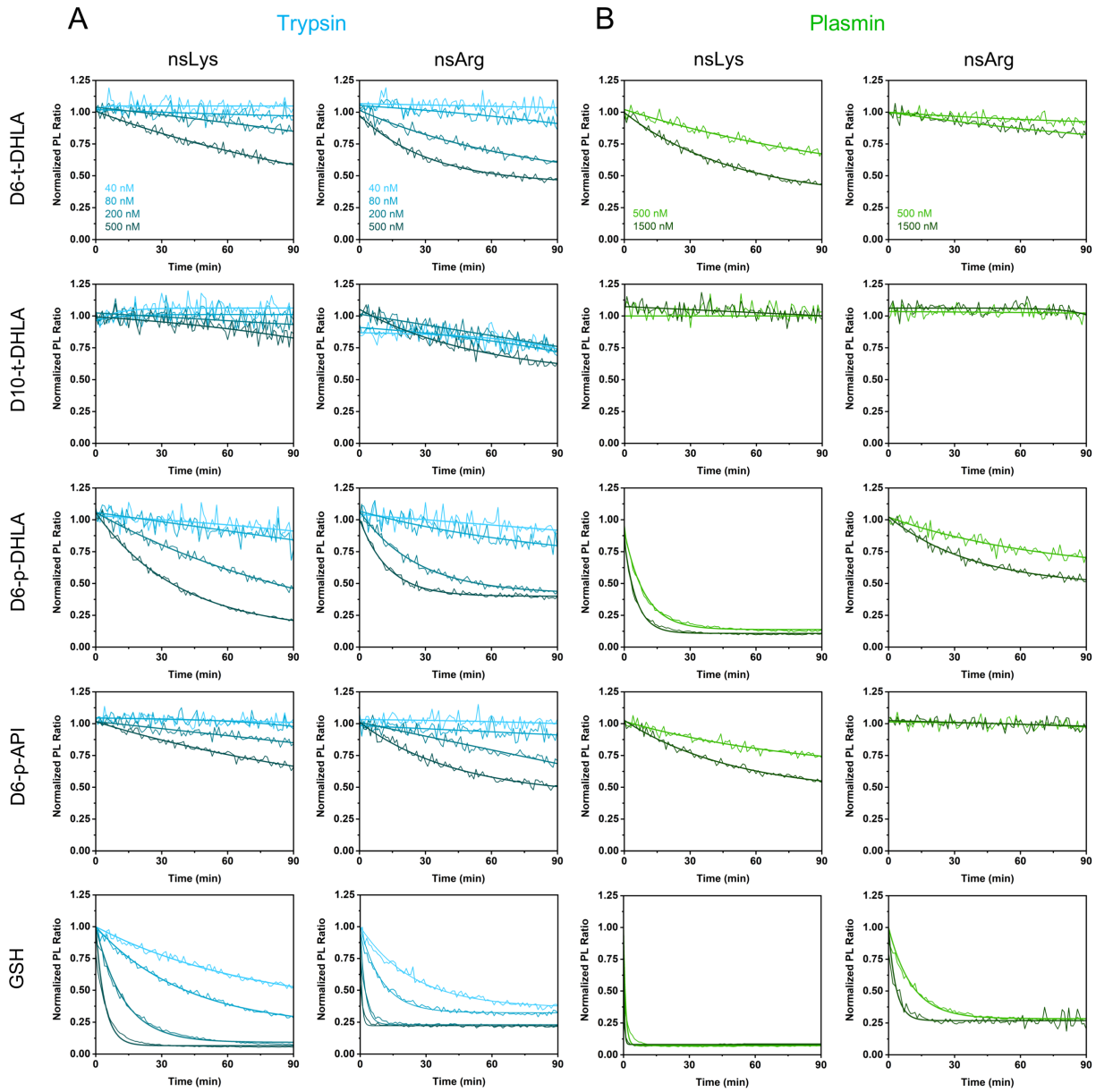

Figure S25. Normalized FRET-based progress curves for **(A)** trypsin-catalyzed hydrolysis of peptide-(X-QD605) conjugates where the peptide substrate is A647-labeled (i) nsLys or (ii) nsArg. See Table S1 for peptide sequences. **(B)** Plasmin-catalyzed hydrolysis of peptide-(X-QD605) conjugates where the peptide substrate is A647-labeled nsLys or nsArg. Each X ligand is across a row. Each peptide substrate is down a column.

Conjugation to Tetrameric Antibody Complexes

Assembly of TAC with QDs

Figure S26 shows an agarose gel of (D10-t-DHLA)-QD645 incubated with different equivalents of TAC. With increasing equivalents of TAC, a decrease in the cathodic mobility was observed, indicating the assembly of TAC on the QDs.

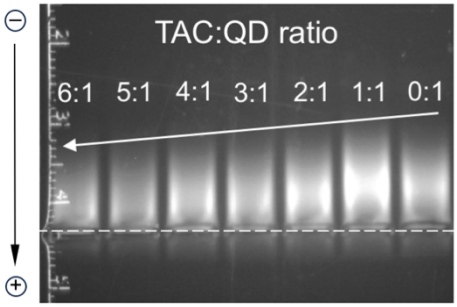

Figure S26. Agarose gel of (D10-t-DHLA)-QD645 incubated with different equivalents of TAC anti-EPO complexes. The decrease in cathodic mobility shows successful binding of TAC to the QDs.

EPO Immunoassay

Figure S27 shows a graph of PL intensity for an EPO immunoassay (Figure 11, main text) done with higher amounts of EPO (5000 mU) in the sample. These results also showed selective binding for EPO with the TAC-QD conjugates. The contrast ratio between EPO and no EPO was 143:1, with a p-value of 0.03.

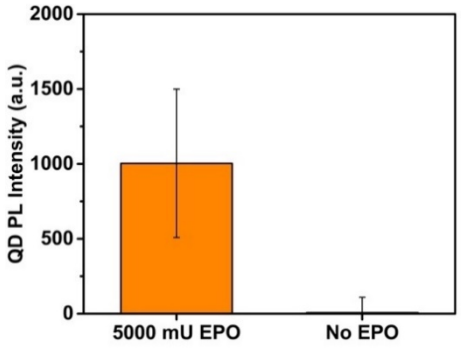

Figure S27. Bar graph of PL intensity for the EPO immunoassay with (D10-t-DHLA)-QD600 in the presence of EPO (5000 mU) and no EPO.

Additional Discussion regarding Protein Adsorption on (D6-p-API)-QDs. The data in Figure 5 (main text) show that protein adsorption on (D6-p-API)-QDs was stronger when compared to QDs functionalized with the other dextran ligands. Additional data are consistent with this conclusion, albeit less directly. With respect to Figure S25, a previous study has shown that plasmin activity is inhibited by non-specific adsorption on QDs.[22] Plasmin-catalyzed hydrolysis of both peptide substrates on (D6-p-API)-QDs was slower than on (D6-p-DHLA)-QDs, although no significant difference in steric hindrance was expected. The same trend was also observed for trypsin, but with a smaller difference in activity, consistent with the previously established lower tendency of trypsin to adsorb on QDs.[22]

Interestingly, microinjection results suggest good intracellular colloidal stability for (D6-p-API)-QDs and poor stability for DHLA, despite both materials doing similarly poorly in the *in vitro* colloidal stability tests in Figure 4 (main text). The distinction is likely that the shortcomings of DHLA were an effect of its distal functional group and not its anchoring to the QD, whereas the situation was likely the opposite for (D6-p-API)-QDs. Proteins in a complex environment (*e.g.* a cell) likely adsorbed and displaced some or all of the D6-p-API ligands and imparted improved colloidal stability, albeit fundamentally changing the surface chemistry.

Supplementary References

(1) Algar, W. R., Blanco-Canosa, J. B., Manthe, R. L., Susumu, K., Stewart, M. H., Dawson, P. E., and Medintz, I. L. (2013) Synthesizing and Modifying Peptides for Chemoselective Ligation and Assembly into Quantum Dot-Peptide Bioconjugates. *Methods Mol. Biol. 1025*, 47–73.

(2) Algar, W. R., and Krull, U. J. (2011) Interfacial Chemistry and the Design of Solid-Phase Nucleic Acid Hybridization Assays Using Immobilized Quantum Dots as Donors in Fluorescence Resonance Energy Transfer. *Sensors 11*, 6214–6236.

(3) Petryayeva, E., and Algar, W. R. (2013) Proteolytic Assays on Quantum-Dot-Modified Paper Substrates Using Simple Optical Readout Platforms. *Anal. Chem. 85*, 8817–8825.

(4) Perez, Y., Valdivia, A., Gomez, L., Simpson, B. K., and Villalonga, R. (2005) Glycosidation of Cu,Zn-Superoxide Dismutase with End-Group Aminated Dextran. Pharmacological and Pharmacokinetics Properties. *Macromol. Biosci. 5*, 1220–1225.

(5) Chen, S., Alves, M. H., Save, M., and Billon, L. (2014) Synthesis of Amphiphilic Diblock Copolymers Derived from Renewable Dextran by Nitroxide Mediated Polymerization: Towards Hierarchically Structured Honeycomb Porous Films. *Polym. Chem. 5*, 5310–5319.

(6) Cohen, J. L., Schubert, S., Wich, P. R., Cui, L., Cohen, J. A., Mynar, J. L., and Fréchet, J. M. J. (2011) Acid-Degradable Cationic Dextran Particles for the Delivery of siRNA Therapeutics. *Bioconjugate Chem. 22*, 1056–1065.

(7) Riddles, P. W., Blakeley, R. L., and Zerner, B. (1979) Ellman's Reagent: 5,5′-Dithiobis(2-Nitrobenzoic Acid)-a Reexamination. *Anal. Biochem. 94*, 75–81.

(8) Riddles, P. W., Blakeley, R. L., and Zerner, B. (1983) Reassessment of Ellman's Reagent. *Methods Enzymol. 91*, 49–60.

(9) Moser, M., Schneider, R., Behnke, T., Schneider, T., Falkenhagen, J., and Resch-Genger, U. (2016) Ellman's and Aldrithiol Assay as Versatile and Complementary Tools for the Quantification of Thiol Groups and Ligands on Nanomaterials. *Anal. Chem. 88*, 8624–8631.

(10) Aldeek, F., Hawkins, D., Palomo, V., Safi, M., Palui, G., Dawson, P. E., Alabugin, I., and Mattoussi, H. (2015) UV and Sunlight Driven Photoligation of Quantum Dots: Understanding the Photochemical Transformation of the Ligands. *J. Am. Chem. Soc. 137*, 2704–2714.

(11) Mishra, D., Wang, S., Michel, S., Palui, G., Zhan, N., Perng, W., Jin, Z., and Mattoussi, H. (2018) Photochemical Transformation of Lipoic Acid-Based Ligands: Probing the

Effects of Solvent, Ligand Structure, Oxygen and pH. *Phys. Chem. Chem. Phys. 20*, 3895–3902.

(12) Wu, M., Petryayeva, E., Medintz, I. L., and Algar, W. R. (2014) Quantitative Measurement of Proteolytic Rates and Förster Resonance Energy Transfer. *Methods Mol. Biol. 1199*, 215–239.

(13) Zylstra, J., Amey, J., Miska, N. J., Pang, L., Hine, C. R., Langer, J., Doyle, R. P., and Maye, M. M. (2011) A Modular Phase Transfer and Ligand Exchange Protocol for Quantum Dots. *Langmuir 27*, 4371–4379.

(14) Han, H., Zylstra, J., and Maye, M. M. (2011) Direct Attachment of Oligonucleotides to Quantum Dot Interfaces. *Chem. Mater. 23*, 4975–4981.

(15) Sjöback, R., Nygren, J., and Kubista, M. (1995) Absorption and Fluorescence Properties of Fluorescein. *Spectrochim. Acta Part A Mol. Spectrosc. 51*, L7–L21.

(16) Hanwell, M. D., Curtis, D. E., Lonie, D. C., Vandermeersch, T., Zurek, E., and Hutchison, G. R. (2012) Avogadro: An Advanced Semantic Chemical Editor, Visualization, and Analysis Platform. *J. Cheminf. 4*, 17.

(17) Pettersen, E. F., Goddard, T. D., Huang, C. C., Couch, G. S., Greenblatt, D. M., Meng, E. C., and Ferrin, T. E. (2004) UCSF Chimera—A Visualization System for Exploratory Research and Analysis. *J. Comput. Chem. 25*, 1605–1612.

(18) Pasika, W. M., and Cragg, L. H. (1963) The Detection and Estimation of Branching in Dextran by Proton Magnetic Resonance Spectroscopy. *Can. J. Chem. 41*, 293–299.

(19) Llamas-Arriba, M. G., Puertas, A. I., Prieto, A., López, P., Cobos, M., Miranda, J. I., Marieta, C., Ruas-Madiedo, P., and Dueñas, M. T. (2019) Characterization of Dextrans Produced by Lactobacillus Mali CUPV271 and Leuconostoc Carnosum CUPV411. *Food Hydrocolloids. 89*, 613–622.

(20) Harris, L. J., Skaletsky, E., and McPherson, A. (1998) Crystallographic Structure of an Intact IgG1 Monoclonal Antibody. *J. Mol. Biol. 275*, 861–872.

(21) Thomas, T. E., Sutherland, H. J., and Lansdorp, P. M. (1989) Specific Binding and Release of Cells from Beads Using Cleavable Tetrameric Antibody Complexes. *J. Immunol. Methods 120*, 221–231.

(22) Petryayeva, E., Jeen, T., and Algar, W. R. (2017) Optimization and Changes in the Mode of Proteolytic Turnover of Quantum Dot–Peptide Substrate Conjugates through Moderation of Interfacial Adsorption. *ACS Appl. Mater. Interfaces 9*, 30359–30372.

(23) Wu, M., and Algar, W. R. (2015) Acceleration of Proteolytic Activity Associated with Selection of Thiol Ligand Coatings on Quantum Dots. *ACS Appl. Mater. Interfaces 7*, 2535–2545.

(24) Jeen, T., and Algar, W. R. (2018) Mimicking Cell Surface Enhancement of Protease Activity on the Surface of a Quantum Dot Nanoparticle. *Bioconjugate. Chem. 29*, 3783–3792.

(25) Maia, J., Ferreira, L., Carvalho, R., Ramos, M. A., and Gil, M. H. (2005) Synthesis and Characterization of New Injectable and Degradable Dextran-Based Hydrogels. *Polymer 46*, 9604–9614.

(26) Kaiser, E., Colescott, R. L., Bossinger, C. D., and Cook, P. I. (1970) Color Test for Detection of Free Terminal Amino Groups in the Solid-Phase Synthesis of Peptides. *Anal. Biochem. 34*, 595–598.

(27) Benoit, D. N., Zhu, H., Lilierose, M. H., Verm, R. A., Ali, N., Morrison, A. N., Fortner, J. D., Avendano, C., and Colvin, V. L. (2012) Measuring the Grafting Density of Nanoparticles in Solution by Analytical Ultracentrifugation and Total Organic Carbon Analysis. *Anal. Chem. 84*, 9238–9245.

(28) Rahme, K., Chen, L., Hobbs, R. G., Morris, M. A., O'Driscoll, C., and Holmes, J. D. (2013) PEGylated Gold Nanoparticles: Polymer Quantification as a Function of PEG Lengths and Nanoparticle Dimensions. *RSC Adv. 3*, 6085–6094.

(29) Rosenberg, K. J., Goren, T., Crockett, R., and Spencer, N. D. (2011) Load-Induced Transitions in the Lubricity of Adsorbed Poly(L-Lysine)-g-Dextran as a Function of Polysaccharide Chain Density. *ACS Appl. Mater. Interfaces 3*, 3020–3025.

(30) Nalam, P. C., Ramakrishna, S. N., Espinosa-Marzal, R. M., and Spencer, N. D. (2013) Exploring Lubrication Regimes at the Nanoscale: Nanotribological Characterization of Silica and Polymer Brushes in Viscous Solvents. *Langmuir 29*, 10149–10158.

(31) Heinze, T., Liebert, T., Heublein, B., and Hornig, S. (2006) Functional Polymers Based on Dextran. In *Polysaccharides II.* Volume 205 (Klemm, D., Ed.) pp 199–291, Springer, Berlin.

(32) Algar, W. R., Jeen, T., Massey, M., Peveler, W. J., and Asselin, J. (2019) Small Surface, Big Effects, and Big Challenges: Toward Understanding Enzymatic Activity at the Inorganic Nanoparticle-Substrate Interface. *Langmuir 35*, 7067–7091.